Exploring the role of High Arctic Large Igneous Province volcanism on Early Cretaceous Arctic forests

Galloway, J. M., Fensome, R. A., Swindles, G. T., Hadlari, T., Fath, J., Schröder-Adams, C., Herrle, J. O., & Pugh, A. (2022). Exploring the role of High Arctic Large Igneous Province volcanism on Early Cretaceous Arctic forests. *Cretaceous Research*, *129*, Article 105022. https://doi.org/10.1016/j.cretres.2021.105022, https://doi.org/10.1016/j.cretres.2021.105022

Published in:
Cretaceous Research

Document Version:
Peer reviewed version

Journal Pre-proof

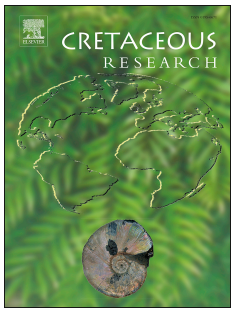

Exploring the role of High Arctic Large Igneous Province volcanism on Early Cretaceous Arctic forests

Jennifer M. Galloway, Robert A. Fensome, Graeme T. Swindles, Thomas Hadlari, Jared Fath, Claudia Schröder-Adams, Jens O. Herrle, Adam Pugh

PII: S0195-6671(21)00270-6

DOI: https://doi.org/10.1016/j.cretres.2021.105022

Reference: YCRES 105022

To appear in: *Cretaceous Research*

Received Date: 7 June 2020

Revised Date: 9 August 2021

Accepted Date: 29 August 2021

Please cite this article as: Galloway, J.M., Fensome, R.A., Swindles, G.T., Hadlari, T., Fath, J., Schröder-Adams, C., Herrle, J.O., Pugh, A., Exploring the role of High Arctic Large Igneous Province volcanism on Early Cretaceous Arctic forests, *Cretaceous Research*, https://doi.org/10.1016/j.cretres.2021.105022.

Author statement for YCRES-S-20-00119

Our CRediT author statement is as follows **Galloway:** conceptualization, methodology, formal analysis, investigation, resources, data curation, writing-original draft preparation, project administration, visualization, project administration, funding acquisition **Fensome:** methodology, formal analysis, investigation, data curation, writing-original draft preparation, visualization **Swindles:** methodology, formal analysis, writing-review and editing **Hadlari:** methodology, investigation, formal analysis, writing-original draft preparation **Fath:** investigation, data curation, writing-review and editing **Schröder-Adams:** conceptualization, methodology, investigation, funding acquisition, writing-review and editing **Herrle:** conceptualization methodology, investigation, funding acquisition, writing-review and editing **Pugh:** investigation, writing-review and editing

Exploring the role of High Arctic Large Igneous Province volcanism on Early Cretaceous Arctic forests

Jennifer M. Galloway[1,2*], Robert A. Fensome[3], Graeme T. Swindles[4], Thomas Hadlari[1], Jared Fath[1,5], Claudia Schröder-Adams[6], Jens O. Herrle[7], Adam Pugh[6,8]

[1]Geological Survey of Canada / Commission géologique du Canada, 3303 - 33 Street N.W. Calgary, Alberta, T2L 2A7, Canada

[2]Aarhus Institute of Advanced Studies, Aarhus University, Aarhus, 8000, Denmark

[3]Geological Survey of Canada / Commission géologique du Canada, Bedford Institute of Oceanography, P.O. Box 1006, 1 Challenger Drive, Dartmouth, NS, B2Y 4A2, Canada

[4]School of Natural and Build Environment, Queen`s University, University Road, Belfast, BT7 1NN, United Kingdom.

[5]Department of Renewable Resources, University of Alberta, Edmonton, AB, T6G 2R3, Canada (current address)

[6]Department of Earth Sciences, Carleton University, Ottawa, ON, K1S 5B6, Canada

[7]Institute of Geosciences, Goethe-University Frankfurt, 60438 Frankfurt am Main, Germany

[8]Cenovus Energy, 225 6 Ave SW, Calgary, AB, T2P 0M5, Canada (current address)

*corresponding author email: Jennifer.Galloway@canada.ca

Abstract

The Hauterivian–Aptian aged Isachsen Formation at Glacier Fiord, Axel Heiberg Island, in the Sverdrup Basin of the Canadian Arctic Archipelago was deposited contemporaneous with

initiation of the High Arctic Large Igneous Province (HALIP). New palynological biostratigraphy and paleoenvironmental reconstruction, in coordination with the emerging geochronology of HALIP igneous rocks, permits exploration of the effects of volcanism on Arctic vegetation during the Early Cretaceous. Four informal terrestrial palynofloral zones are defined and used to reconstruct vegetation change over the Isachsen Formation's ca. 17 million year history and explore the role of the HALIP in these changes. Climate warming during the Hauterivian promoted expansion of a hinterland community dominated by members of the Pinaceae. By the middle Barremian, this community was replaced by mixed heathland and mire, represented by up to 70% fern spores in the uppermost Paterson Island Member,that may be, in part, in response to environmental disturbance associated with volcanic flows of the HALIP. Above the fern spore spike, dinoflagellate cyst assemblages suggest an early Aptian age and a marine setting for mudstones of the Rondon Member in which Ocean Anoxic Event 1a is recorded. An interval of floral instability is recorded in the overlying Walker Island Member, characterized by fluctuations in Pinaceae and Cupressaceae pollen and fern spores, possibly as a result of post-OAE 1a temperature variabilty and landscape disturbance associated with lava flows of the HALIP that were repeatedly extruded onto the subsiding delta plain during deposition of the member.

Keywords

Cretaceous; Arctic; Palynology; Paleoecology; High Arctic Large Igneous Province; OAE 1a

1.0 Introduction

The Cretaceous Period is generally considered to have been a time of warm and equable greenhouse climate (e.g., Föllmi, 2012). This is attributed mainly to high partial pressure of carbon dioxide (~700->4000 ppmv; Bice and Norris, 2002) as a result of elevated background rates of volcanic degassing (e.g., Larson, 1991). However, recent research shows that a number of cooling events punctuated otherwise warm climatic conditions of this interval in the planet's history (e.g., Kemper, 1975; Frakes and Francis, 1988; Price, 1999; McAnena et al., 2013; Galloway et al., 2015; Herrle et al., 2015; Jenkyns et al., 2017; Grasby et al., 2017; Rogov et al., 2017; Vickers et al., 2019). These cooling events may even have caused transient glacial conditions in high northern latitudes (Price and Nunn, 2010; Vickers et al., 2019). The forcing mechanisms of some Cretaceous climatic perturbations may have been related to carbon drawdown associated with the construction and destruction of one or more large igneous provinces (LIPs) (Erba and Tremolada, 2004; Jenkyns et al., 2017; Beil et al., 2020). For example, the High Arctic and Caribbean LIPs, Ontong Java Plateau, and Madagascar Flood Basalts are implicated in the genesis of Ocean Anoxic Event 2 and cooling associated with the Plenus Cold Event (Jenkyns et al., 2017). The release of CO_2 associated with emplacement of LIPs coupled with weathering of newly extruded basalt may have led to elevated nutrient levels and planktonic productivity in global oceans multiple times during the Cretaceous, periodically resulting in widespread ocean anoxia (e.g., Erba, 1994; Jarvis et al., 2011; Jenkyns et al., 2017; Jenkyns, 2018). The ensuing carbon burial associated with ocean anoxic events (OAEs) and silicate weathering of newly exposed LIPs are important mechanisms of drawdown of atmospheric carbon dioxide that, in the absence of replenishment, ultimately led to transient global cooling (Jarvis et al., 2011; Jenkyns et al., 2017). Thus, LIPs are important drivers for sequences of biogeochemical events that affect global climate.

The High Arctic Large Igneous Province (HALIP) was a protracted event lasting more than 40 myr but is probably the least studied of all known LIPs (Saumur et al., 2016). There were two dominant pulses (Maher, 2001; Ernst, 2014; Jowitt et al., 2014): a tholeiitic phase of magmatism that began as early as 127 Ma and peaked at 122 Ma, followed by an alkaline phase that started at ca. 94 Ma in Canada and later in Greenland at ca. 85 Ma in Greenland (Estrada and Henjes-Kunst, 2004, 2013; Tegner et al., 2011; Evenchick et al., 2015). Polteau et al. (2016) and Planke et al. (2017) speculated that carbon mobilization associated with the Barents Sea Sill Complex (part of the HALIP) could have triggered OAE 1a and its associated negative $\delta^{13}C$ excursion in the early Aptian. Schröder-Adams et al. (2019) considered that methane release associated with the HALIP contributed to the rapid global warming that led to OAE 2 at the end of the Cenomanian.

Polar regions are highly sensitive to changes in climate forcing (Holland and Bitz, 2003) and are important in global climate feedback mechanisms, at present and in the geological past (Poulson and Zhou, 2013). High northern latitudes were covered with dense coniferous forests during the Early Cretaceous despite extreme photic seasonality (Galloway et al., 2013, 2015). The composition and extent of terrestrial vegetation plays an important role in climate feedback (Woodward, 1998), but information on the role and response of high northern latitude terrestrial plant communities to Mesozoic climate variability is sparse relative to lower latitudes (Spicer and Parrish, 1986; Gröcke et al., 2005; Harland et al., 2007; Selmeier and Grosser, 2011; Galloway et al., 2012, 2013, 2015). Moreover, few studies have evaluated the effects of LIPs on terrestrial vegetation despite the importance of terrestrial ecosystems in the carbon cycle (e.g., Jolley, 1997; Jolley et al., 2008; Ebinghaus et al., 2015), and none have explored the effects of the HALIP on Arctic forests.

The Sverdrup Basin in the Canadian Arctic (Fig. 1) contains a nearly continuous succession of Lower Cretaceous strata (Fig. 2). During the Jurassic and Cretaceous, the Sverdrup Basin was extensional and separated from the developing Amerasia Basin by a paleohigh, possibly a horst-like rift shoulder, called the Sverdrup Rim (Meneley et al., 1975; Embry and Dixon, 1990; Hadlari et al., 2016). The upper Valanginian to lower Aptian Isachsen Formation of the Sverdrup Basin is a unit of particular interest from a tectonic and paleoclimatic perspective because it was deposited in marine, deltaic, and fluvial environments during the development of the adjacent Amerasia Basin (Embry and Dixon, 1990; Tullius et al., 2014) and contains a well-preserved mainly terrestrial fossil record (Galloway et al., 2015). During Jurassic to earliest Cretaceous rift-related subsidence in the Sverdrup Basin, space was created for the Jameson Bay Formation to the Deer Bay Formation succession, with maximum subsidence during deposition of the Deer Bay Formation. The Isachsen Formation was then deposited and represents the post-rift succession and contains the breakup unconformity associated with the formation of the Amerasia Basin (Hadlari et al., 2016; Fig. 2). Deposition of the Isachsen Formation is contemporaneous with initiation of the HALIP at ca. 127 Ma and its main pulse at ca. 122 ± 2 Ma (Dockman et al., 2018 and references therein). The HALIP likely played a role in environmental change during the Early Cretaceous (Polteau et al., 2016; Planke et al., 2017; Schröder-Adams et al., 2019). Study of the Isachsen Formation can thus provide insight into the role of tectonism and volcanism associated with the HALIP on the Cretaceous Arctic biome. However, a lack of biostratigraphic characterization of the Isachsen Formation poses a challenge for understanding Cretaceous geology of the Canadian Arctic in general (e.g., Evenchick et al., 2019) and limits understanding of the chronology and environmental effects of the HALIP in particular. Herein, the integration of a biostratigraphic and carbon isotopic (Herrle et al., 2015) framework in coordination with the emerging geochronology

of HALIP igneous rocks permits exploration of the consequences of Arctic volcanism on Early Cretaceous climate and terrestrial ecosystems.

2.0 Regional setting

2.1 Sverdrup Basin

The Sverdrup Basin is a 1300 km by 350 km paleo-depocentre in the Canadian Arctic Archipelago (Fig. 1). Developed through subsidence and rifting that began during the early Carboniferous (Thorsteinsson, 1974), the basin contains an up-to-13 km-thick succession of nearly continuous strata as young as Paleogene (Balkwill, 1978; Embry and Beauchamp, 2019; Figs. 1, 2). Rifting continued through the late Carboniferous, resulting in widespread flooding and increasingly open-marine connections with Panthalassa to the west and seas that covered northern Greenland and the present-day Barents Sea region to the east (Embry and Beauchamp, 2019). Another major episode of rifting began by the Early Jurassic, the later stages of which were associated with the opening of the Amerasia Basin. Rifting peaked during deposition of the Deer Bay Formation, and the lowermost Isachsen Formation represents deltaic progradation across the basin when rift-related subsidence had slowed, marking the early post-rift stage (Hadlari et al., 2016). In the adjacent Amerasia Basin, rifting during the Jurassic to earliest Cretaceous progressed to sea-floor spreading by the Early Cretaceous, as inferred from the breakup unconformity in the post-rift succession of the Sverdrup Basin (Hadlari et al., 2016; Embry and Beauchamp, 2019), most likely marking the onset of sea-floor spreading in the proto-Arctic Ocean. Sedimentation in the Sverdrup Basin was then dominated by terrigenous clastic material that recorded basin-wide

transgressive-regressive cycles driven by a combination of tectonism, sediment supply, and eustatic sea-level change (Embry, 1991). Deposition in the Sverdrup Basin ended during the Paleogene as a consequence of regional compression and widespread uplift during the Eurekan Orogeny (Embry and Beauchamp, 2019). Strata in the Sverdrup Basin are deformed due to several factors: episodic flow of Carboniferous evaporites during the Mesozoic (Balkwill, 1978; Boutelier et al., 2010; Galloway et al., 2013; Dewing et al., 2016), Barremian to Cenomanian magmatism and faulting (Embry and Osadetz, 1988; Embry, 1991), and compression during the Eurekan Orogeny in the Eocene. The Eurekan Orogeny produced high amplitude folds and thrust faults in northeastern parts of the basin and smaller folds to the west (Harrison et al., 1999).

The age of Mesozoic strata in the Sverdrup Basin is based primarily on ammonoids, bivalves, dinoflagellate cysts (dinocysts), radiolarians, and foraminifers (e.g., Frebold, 1960, 1975; Tozer and Throsteinsson, 1964; Jeletzky, 1973; Hopkins, 1971, 1973; Balkwill, 1983; Wall, 1983; Nøhr-Hansen and McIntyre, 1998; Schröder-Adams et al., 2014; Pugh et al., 2014; see Galloway et al., 2013, 2015, 2019 for more complete literature) and supplemented by carbon isotope stratigraphy (Herrle et al., 2015; Galloway et al., 2019; Dummann et al., 2021), as part of an emerging geochronological framework (Omma et al., 2011; Estrada and Henjes-Kunst, 2013; Schröder-Adams et al., 2014; Evenchick et al., 2015; Herrle et al., 2015; Midwinter et al., 2016; Anfinson et al., 2016; Davis et al., 2016; Hadlari et al., 2016; Dockman et al., 2018; Kingsbury et al., 2018; Evenchick et al., 2019; Fig. 2).

Axel Heiberg Island is located in the Canadian Arctic Archipelago, in the west-central part of Sverdrup Basin, near the basin's axis. It was situated between paleolatitudes 74 ± 2˚ (standard error) and 79 ± 1˚ during the Early Cretaceous (Wynne et al. 1988). Glacier Fiord on southern Axel Heiberg Island (Fig. 1) was targeted for detailed study due to preservation at this location of

159 an exceptionally well-exposed succession of the Isachsen Formation (Schröder-Adams et al., 2014;
160 Dummann et al., 2021).
161
162 *2.2 Isachsen Formation*
163
164 2.2.1 Lithostratigraphy of the Isachsen Formation
165
166 The Isachsen Formation was first described, on Ellef Ringnes Island, by Heywood (1957)
167 as a succession of arenaceous strata between the mudstones and siltstones of the underlying Deer
168 Bay Formation and overlying Christopher Formation (Fig. 2). The Isachsen Formation is
169 widespread throughout the Sverdrup Basin, ranging in thickness from ~120 m at the basin margins
170 to 1370 m on western Axel Heiberg Island (Hopkins, 1971).
171 The Isachsen Formation is subdivided into three members based on gamma-log
172 interpretation of wire-line data from the Skybattle Bay C-15 well (Lougheed Island; 77º14'N,
173 105º05'W; Embry, 1985; Fig. 2). The Paterson Island Member overlies the Deer Bay Formation
174 unconformably at basin margins and conformably in the basin centre. The Paterson Island Member
175 consists of fine- to very coarse-grained sandstone with interbeds of mudstone, siltstone, coal, and
176 volcanic and volcaniclastic/tuffaceous rocks (Embry and Osadetz, 1988; Evenchick and Embry,
177 2012a,b) deposited in a delta plain setting with fluvial environments (Embry, 1985). The
178 coarsening-upward cycles in the basal portion of the member in basinal sections (e.g., on Ellef
179 Ringnes Island) are of delta front origin (Embry, 1985; Tullius et al., 2014). Sandstone units are
180 up to 35 m thick, and argillaceous intervals 2–10 m thick occur in the 152 m-thick type section in
181 Skybattle Bay C-15 well (Embry, 1985). The Paterson Island Member is conformably overlain by

interbedded medium- to dark-grey siltstone of the Rondon Member, which was deposited in a marine-shelf setting (Embry 1985; Nøhr-Hansen and McIntyre, 1998; Tullius et al., 2014). The type section in the Skybattle C-15 well is 47 m thick (Embry, 1985). The second largest accumulation of oil in the Sverdrup Basin was discovered in 1980 during drilling of the Panarctic Balaena D-58 well off Ellef Ringnes Island, where the Paterson Island Member is an oil and gas reservoir, with the Rondon Member acting as a seal (Waylett and Embry, 1992). The Rondon Member is conformably overlain by interbedded fine- to coarse-grained sandstone, siltstone, and minor coal of the Walker Island Member. The type section of the Walker Island Member in the Skybattle C-15 well is 140 m thick (Embry, 1985). The Walker Island Member is composed of marginal marine, bioturbated and fluvial sandstones with mud-drapes indicating tidal influence and was deposited in a delta front to delta plain environment (Embry 1985; Tullius et al., 2014). The Walker Island Member is conformably overlain by mudstones, siltstones, and fine-grained sandstones of the Christopher Formation.

2.2.2. Age of the Isachsen Formation

The age of the Isachsen Formation is summarized in Suppl. 1 and ranges from late Valanginian to early Aptian. This interpretation is based on the age of bounding strata and limited fossil evidence. The age of the underlying Deer Bay Formation ranges from Tithonian to Valanginian (Galloway et al., 2019 and references therein), while the age of overlying Christopher Formation ranges from Aptian to Albian (Schröder-Adams et al., 2014; Herrle et al., 2015). The base of the Paterson Island Member is diachronous; it may be as old as late Valanginian and extends into the early or middle Barremian (Embry, 1985), or early Aptian (Herrle et al., 2015;

Dummann et al., 2021). Dinocysts preserved in the Rondon Member exposed at Glacier Fiord and Buchanan Lake on Axel Heiberg Island, and from south Sabine Peninsula on Melville Island, have been used to interpret a Barremian age for this marine unit (Costa, 1984; McIntyre, 1984; McIntyre pers. comm. 1984 in Embry, 1985, 1991; Nøhr-Hansen and McIntyre, 1998; Suppl. 1). However, comparison of carbon isotope stratigraphy of the Isachsen Formation at the Glacier Fiord on Axel Heiberg Island with a composite Tethyan curve provides convincing evidence for an early Aptian age of the Rondon Member because of the distinctive negative shift in $\delta^{13}C_{org}$ associated with OAE 1a (Herrle et al., 2015), as well as individual carbon isotope segments (CIS) that can be related precisely to well-dated reference curves of lower latitudes (Dummann et al., 2021). Therefore, the dinocyst-based age determinations are herein revisited. Based on the age of the Rondon Member and overlying Christopher Formation, the age of the Walker Island Member is inferred to be either Barremian to Aptian (Embry, 1985) or entirely Aptian (Herrle et al., 2015; Dummann et al., 2021). The uncertainty in the age of the Isachsen Formation and its members poses a challenge for understanding Lower Cretaceous rocks of the Sverdrup Basin (Evenchick et al., 2019).

2.2.2 Sequence stratigraphy of the Isachsen Formation

Four sequences are recognized in the Isachsen Formation (Galloway et al., 2015). Sequence 1 represents Valanginian strata of the lower Paterson Island Member and is preserved in the central Sverdrup Basin on Ellef Ringnes Island, and has typically been eroded in the eastern parts of the basin (Galloway et al., 2015). This sequence represents progradation of a delta when tectonic subsidence had slowed, designated as early post-rift (Hadlari et al., 2016). This bioturbated succession is absent from outcrops of Isachsen Formation at Glacier Fiord due to uplift associated

with crustal breakup in the adjacent Amerasia Basin and possibly thermal doming associated with the first pulses of the HALIP (Vickers et al., 2016). The base of sequence 2 represents the widespread sub-Hauterivian unconformity associated with breakup in the adjacent Amerasia Basin, and it truncates early post-rift strata of the lowermost Paterson Island Member at many localities in the Sverdrup Basin (Galloway et al., 2015; Hadlari et al., 2016). Above the unconformity are cross-bedded fluvial sandstones of the middle part of the Paterson Island Member. These sandstones grade upward into finer-grained non-marine deposits consisting of fining-upward sandstones interbedded with siltstone, mudstone, and coal, herein informally termed the Paterson Island shale (Galloway et al., 2015), indicating deposition in a floodplain setting with overbank and channel environments (Embry, 1985; Tullius et al., 2014). Sequence 3 in the Isachsen Formation is represented by fining upward successions of sandstone deposited in a fluvial environment during the late Barremian and forming the uppermost strata of the Paterson Island Member. These fluvial sandstones correlate across the northern part of the Sverdrup Basin above the Paterson Island shale (Tullius et al., 2014; Galloway et al., 2015), and are interpreted here to be at the base of the sequence that grades upward to the Rondon Member. The Rondon Member was deposited in a marine environment and is interpreted by Herrle et al. (2015) and Dummann et al. (2021) to be of early Aptian age at the Glacier Fiord locality. The marine deposits of the Rondon Member grade upward into shoreface to local fluvial facies of the lower Walker Island Member. The transition from regression to transgression in the upper part of the Walker Island Member, which is Aptian in age (Suppl. 1), marks the boundary at the base of a fourth sequence. The marine sandstones forming the lower part of this sequence represents a shoreline to shallow-marine setting and reflect an overall transgressive succession that continues into the lower Christopher Formation.

2.2.3 Previous work on the Isachsen Formation

Initial terrestrial palynological research on the Isachsen Formation in the Sverdrup Basin by Hopkins (1971) qualitatively described palynoflora preserved in samples collected from the bottom of seismic shot-holes on northwestern Melville Island to provide age control for the unit. Galloway et al. (2013) quantitatively examined seven samples from the Isachsen Formation for pollen and spores as part of a study of a longer stratigraphic succession preserved in the Hoodoo Dome H-37 oil and gas well, southern Ellef Ringnes Island. Palynoflora show that an episode of relatively cool and moist conditions punctuated an otherwise warm climate during the late Valanginian to early Hauterivian. In a more detailed facies and palynological study of the formation based on three outcrop sections exposed on Ellef Ringnes Island in the central Sverdrup Basin, Tullius et al. (2014) and Galloway et al. (2015) interpreted the following three climatic phases: a relatively cool and moist Valanginian interval; a relatively warmer interval in the Hauterivian; and a return to cool and moist conditions in the Barremian. However, in these previous studies the marine strata of the Rondon Member were either lacking (Galloway et al. 2013) or samples from the Rondon Member were barren of palynomorphs (Tullius et al., 2014; Galloway et al., 2015). Moreover, the Ellef Ringnes Island sections of the Isachsen Formation were incomplete due to local uplift associated with salt diapirism (Galloway et al., 2015). The exceptionally well-exposed and well-constrained outcrop succession from Glacier Fiord, Axel Heiberg Island, in the central-eastern part of the Sverdrup Basin, is employed here as a reference section to refine the understanding of the biostratigraphy, paleoclimate, and terrestrial-vegetation response to environmental perturbations associated with the HALIP. Carbon isotope stratigraphy

from this section has indicated that the age of the marine Rondon Member is early Aptian rather than Barremian (Herrle et al., 2015; Dummann et al., 2021). This is a significant finding in the context of relative dating of the first extrusive components of the HALIP in the absence of geochronology on minerals within the basaltic flows. Age control of the Isachsen Formation is herein explored using dinocyst biostratigraphy and quantitatively-defined pollen and spore assemblage zones.

2.2.4 The High Arctic Large Igneous Province and the Isachsen Formation

Basalt flows within the Isachsen Formation represent the first pulses of extrusive volcanism associated with the HALIP. The age of these flows is based on limited geochronology (summarized in Dockman et al., 2018) and therefore interpretation of their age is usually based on their stratigraphic position relative to the Rondon Member, where dinocyst ranges can be compared with known regionally and globally established ranges of species that have been calibrated in various ways. The position of the flows are based on lithostratigraphic height relative to the Rondon Member (Embry and Osadetz, 1988), or occasionally only as "above" or "below" the member (Evenchick et al., 2012). In the absence of geochronology, paleontology, and/or chemostratigraphy, interpretations of the age of the flows can be problematic (Evenchick et al., 2015, 2019). In some cases, reports of HALIP "flows" have been re-interpreted as intrusive rocks (Bédard et al., 2016; Evenchick et al., 2019), which changes their age interpretations significantly.

The oldest U-Pb age for the initiation of HALIP is 126.6 ± 1.2 Ma from a gabbroic sill on Ellef Ringnes Island that intruded into an undetermined member of the Iscashen Formation (see Evenchick et al., 2012, fig. 12). The first main pulse of igneous activity associated with the HALIP,

297 however, was centred later, at 122 ± 2 Ma (Dockman et al., 2018). Collectively, the ages of the
298 first pulse of the HALIP, that, with error, span from 127.8 Ma to 120 Ma, therefore bracket the
299 Barremian-Aptian boundary of 121.4 (Gale et al., 2020). These ages thus accord with both the
300 previous Barremian age attribution and the Aptian age attribution of the Rondon Member proposed
301 by Herrle et al. (2015) and Dummann et al. (2021) at Glacier Fiord based on carbon isotope
302 stratigraphy. The Rondon member overlies the Paterson Island Member and its associated volcanic
303 rocks. Whereas the volcanic flows in the Paterson Island Member are not dated, they are likely
304 broadly contemporaneous with the dated intrusions.

305 Volcanic flows that occur in the Paterson Island Member are known from two localities:
306 the Geodetic Hills on east-central Axel Heiberg Island and Bjarnason Island (Tozer, 1963). In the
307 Geodetic Hills, a single 10.5 m-thick basalt flow interbedded with coarse-grained fluvial sandstone
308 of the Paterson Island Member occurs 125 m below the Rondon Member (Embry and Osadetz,
309 1988). We herein report from our own field observations at Geodetic Hills in 2015 (Thomas
310 Hadlari) that these are pillowed flows and confirm the volcanic interpretation. The age of the flow
311 was interpreted to be late Hauterivian to middle to late Barremian by Embry and Osadetz (1988)
312 based on interpretation of the age of the Rondon Member as middle to late Barremian and the
313 position of the flow below the Rondon Member. Two basalt flows, each about 10 m thick, are
314 present in the Paterson Island Member at Bjarnason Island (Tozer, 1963). The stratigraphic
315 position of these flows similarly suggested a late Hauterivian or early Barremian age to Embry and
316 Osadetz (1988), but could be as young as early Aptian based on the revised age of the Rondon
317 Member of Herrle et al. (2015).

318 A second episode of volcanism is preserved in the Walker Island Member of the Isachsen
319 Formation. Volcanic rocks of this episode have been documented from the following areas, as

summarized by Embry and Osadetz (1988) and Evenchick et al. (2019): northwestern Axel Heiberg Island, between Middle Fiord and Bunde Fiord (McMillan, 1963; Tozer, 1963; Fischer, 1985); central Axel Heiberg Island, near the head of Strand Fiord, the Geodetic Hills, and the mouth of Mokka Fiord (Fricker, 1963; Tozer, 1963; Thorsteinsson, 1971; Ricketts, 1985); and northwestern Ellesmere Island, in the valley between the Blue and Backwelder mountains (Thorsteinsson, 1971; Moore, 1981). Embry and Osadetz (1988) described a 28 m-thick volcanic unit consisting of three flows at the mouth of Mokka Fiord; they tentatively assigned it to the Walker Island Member because they interpreted the host sandstones to be overlain by Christopher Formation shales, and because the flow had reversed polarity (Wynne et al., 1988). In the Blue Mountains region of northwestern Ellesmere Island, a basalt unit up to 20 m thick lies near the top of the Isachsen Formation, just a few metres below the Christopher Formation (Moore, 1981; Embry and Osadetz, 1988). The rocks at Mokka Fiord are reinterpreted by Evenchick et al. (2019) to be a sill rather than a flow and the rocks at Blue Mountains are now considered also to be sills (Bédard et al., 2016).

Embry and Osadetz (1988) measured a 300 m-thick section of the Walker Island Member in the Bunde Fiord region that consists of up to 220 m of basalt flows, with interbedded quartzose sandstone and pyroclastic and epiclastic volcanic sediments. Individual flows are 5 to 30 m thick, columnar-jointed, amygdaloidal, and commonly contain abundant petrified wood fragments and tree stumps up to 60 cm long. The sandstone units of the Walker Island Member are fluvial and thick-bedded, and are commonly trough or planar cross-bedded and have basal granule and cobble lags. Volcanic fragments and grains are absent from these thick sandstone beds, although they are present in some thin sandstone beds associated with siltstones, coals, and mudstone that occur at the top of the thick sandstone beds. Embry and Osadetz (1988) further described a persistent unit

that is approximately 20 m thick and composed of poorly stratified lahars, thin-bedded volcanic granulestone, and lithic sandstone. This unit occurs near the top of the Isachsen Formation and commonly below the uppermost volcanic flows. A thin-bedded, fine-grained quartz sandstone, approximately 1 m thick, occurs on top of the uppermost flow and thus constrains the volcanic rocks to be within the Walker Island Member of the Isachsen Formation rather than the lowermost beds of the overlying Christopher Formation. At Li Fiord, a similar section of the Walker Island Member was documented by Embry and Osadetz (1988) that is 125 m thick. At the Geodetic Hills, east-central Axel Heiberg Island, three basalt flows with a combined thickness of 11 m occur in the Walker Island Member. The most southerly location of volcanic strata in the Walker Island Member occurs at the head of Strand Fiord, where an 80 m-thick unit of basalt breccia occurs near the top of the member (Ricketts, 1985; Embry and Osadetz, 1988). All of the flows in the Walker Island Member are interbedded with clastic sediments of fluvial origin, and are thus interpreted as being extruded onto subsiding delta plains (Embry and Osadetz, 1988). Embry and Osadetz (1988) inferred all of the basaltic flows in the Walker Island Member as being of late Barremian to Aptian age on the basis of their stratigraphic position above the Rondon Member and below the Christopher Formation, the latter being of late Aptian to early Albian age (Schröder-Adams et al., 2014). Herein, the age of the Walker Island Member basaltic flows are re-interpreted to have a maximum early Aptian age based on the revised age of the underlying Rondon Member (Herrle et al., 2015).

3.0 Material and methods

Cretaceous strata exposed at Glacier Fiord are over 3 km thick and include the Isachsen Formation, which is approximately 0.5 km thick. In 2011 the lithology of the Isachsen Formation was logged, including its contacts with underlying Deer Bay Formation and overlying Christopher Formation, and sampled material for palynological analyses (Fig. 3).

3.1 Palynology

Fifty-six samples were collected from coal, mudstone, and siltstone of the Isachsen Formation for palynological analysis (Table 1, Fig. 3).

Samples were prepared for palynology following standard extraction techniques (Traverse, 2007) at the Geological Survey of Canada (Calgary). The process included washing, acid digestion, oxidation with Schulze's solution, and staining with Safranin O; residues were mounted with polyvinyl and liquid bioplastic. A quantitative approach was used for terrestrial palynomorphs to evaluate the paleoecological effects of the HALIP on land plants. Observations of terrestrial palynomorphs were made by Jennifer M. Galloway at the Geological Survey of Canada (Calgary) using an Olympus BX61® transmitted light microscope with oil immersion at 400x and 1000x magnification. Digital images were captured using an Olympus DP72 camera and Stream Motion® software. A qualitative approach was used for dinocyst evaluation for the purpose of biostratigraphic age determination. This work was carried out by Robert A. Fensome at the Geological Survey of Canada (Atlantic) using a Zeiss Axioplan 2® transmitted light microscope. Photographs were made using a Phase 2 Plan Neofluar 40 x 0.75 lens and Nikon D90 camera body custom-mounted onto the microscope. Thirty-two of the 57 samples yielded sufficiently well-preserved and abundant terrestrial palynomorphs for quantitative analyses (Fig. 3; Table 1).

Quantitative analyses of palynomorphs are based on counts of unsieved preparations with mostly greater than 300 spores and pollen enumerated per sample. The +45 µm size fraction of a selection of these 32 preparations plus additional samples were evaluated for age-diagnostic dinocysts (Table 1).

Rock samples, prepared residues, and microscope slides are stored at the Geological Survey of Canada, Calgary, Alberta, on loan from the Government of Nunavut.

3.2 Multivariate statistical analysis

Multivariate statistical analyses were used on quantitative assessment of the terrestrial pollen and spores (mean 277 ± 69 SD, *n*=32 samples; total 3634 terrestrial pollen and spores enumerated; Suppl. 2). The relative abundance of each taxon is based on a sum that includes palynomorphs with affinities to terrestrial land plants. Non-terrestrial palynomorphs, including dinocysts, algae, acritarchs, and reworked palynomorphs were also enumerated but excluded from the pollen and spore sum; their abundance is expressed as a proportion of the terrestrial pollen and spore sum. The relative abundance of these non-pollen palynomorphs (mean dinocysts 3% ± 9 SD, *n*=32; mean acritarchs 0.1% ± 0.5 SD; mean algae 0.2% ± 0.3 SD; mean undifferentiated non-pollen-palynomorphs 0.3% ± 0.9 SD) and reworked pollen and spores (mean 0.2% ± 0.7 SD) are included in the multivariate analyses but are unlikely to make a large impact on the results due to their low abundances.

Changes in the relative abundance of plant groups at the order level (Suppl. 3), where possible, were explored using multivariate statistical techniques. The order to which the extinct family Cheirolepidaceae was related to is unknown; family level classification is therefore used

for this gymnosperm taxon. We use the informal term bryophyte to encompass three divisions of non-vascular land pants, the liverworts (Marchantiophyta), hornworts (Anthocerotophyta), and mosses (Bryophyta), because the majority of spores encountered in the Isachsen Formation material have unknown or poorly known taxonomic affinities at the order level. Taxa with uncertain affinities up to and including the order level are grouped as *incertae sedis*. These taxa include: *Aequitriradites verrucosus*, *Foraminisporis dailyi*, *Triporoletes reticulatus* (putatively of the order Marchantiopsida), *Matthesisporites tumulosus*, and *Sestrosporites pseudoalveolatus* (Suppl. 3). Collectively taxa of uncertain affinity are a low proportion of the total palynomorph assemblage (mean 0.3 % ± 0.5 SD, *n*=32).

Ordination techniques are commonly used in ecology and paleoecology to determine major gradients in taxa composition that can be linked to environmental and ecological factors that control assemblage composition. Ordination techniques are operations on a community data matrix (e.g., taxa by sample matrix) whereby taxa and/or samples are arranged (ordinated) along gradients, and is used to represent species relationships in low-dimensional space whereby the most important and interpretable environmental gradients may be inferred. This is also a method whereby community level patterns may become evident (Gauch, 1982). Ordination is a particularly useful method to explore paleontological data because fossil assemblages may represent discrete communities, gradients in which taxa are distributed individualistically according to environmental preferences, and/or an association of community signatures transported and preserved in a geologic deposit (Springer and Bambach, 1985; Bambach and Bennington, 1996; Bennington and Bambach, 1996; Holland et al., 2001; Bush and Balme, 2010). Non-metric multi-dimensional scaling (NMDS) is used to compare potential dissimilarity of palynomorph content of stratigraphic levels in the Isachsen Formation at Glacier Fiord and to reduce the multivariate

data to two dimensions to facilitate ecological interpretation. NMDS was performed using the computer program R and the package 'vegan' (R Core Team, 2017; Oksanen et al. 2017). The Bray-Curtis dissimilarity calculation was used. Reworked and indeterminated palynomorphs (palynomorphs of uncertain affinity up to and including the order level), and non-pollen palynomorphs are also included in NMDS. Stress was <0.2 which was deemed "good". We integrate NMDS with Q- and R-mode cluster analysis using Ward's minimum variance method and relative Euclidean distance performed using the computer program SYSTAT to determine if a palynological signature for lithostratigraphic units of the Isachsen Formation could be determined.

Q-mode clusters, and the orders of taxa that compose them, were then graphed stratigraphically using the Tilia and TGView computer programs (Grimm, 1993-2001) to view changes over time at the assemblage scale. Stratigraphically constrained cluster analysis using incremental sum of squares (CONISS; Grimm, 1987) was applied to square-root transformed (to up-weigh rare types, partially reduce problems associated with closed sum percentage data, to improve normality, and because it is highly recommended when using count variables (Sokal and Rohlf, 1995) relative abundance of each order of obligately terrestrial plants to delineate major changes in palynoassemblages over time. Reworked and unidentified palynomorphs and non-pollen palynomorphs were not included in CONISS cluster analysis.

4.0 Results

Of the 57 horizons sampled for palynology, only 32 were sufficiently productive for quantitative analyses of palynomorphs. These samples contain pollen, spores, dinocysts, algae,

and acritarchs assigned to 96 taxa (Figs. 4, 5; Suppl. 4). Preservation ranges from exceptional to poor in the productive samples (Figs. 4, 5).

4.1 Dinocysts

In the quantitative analysis of unsieved preparations for terrestrial pollen and spores analysis, dinocysts are rare (<1%) in most samples except those of the Rondon Member, where dinocysts make up to 42% of the assemblage (sample B-36). In the uppermost Walker Island Member (B-56) dinocysts represent 4% of the assemblage. Samples qualitatively analyzed for dinocysts from the uppermost Paterson Island Member and Rondon Member yield a diverse assemblage (Suppl. 4).

Qualitative analysis of dinocysts was conducted in addition to quantitative analysis to improve the age control and determine if fully marine conditions prevailed during deposition of the Rondon Member. For all but one of the samples attributed to the Paterson Island Member, no dinocysts were found. The one exception is sample B-34, the sample immediately below the first sample tentatively considered to belong to the Rondon Member based on field observations. Rare dinocysts in this uppermost Paterson Island Member sample included *Oligosphaeridium pulcherrimum* and *Vesperopsis*? sp., neither of which are helpful biostratigraphically in the present context. The suite of samples that followed (B-35 to B-38) contain dinocysts that suggest neritic marine conditions from their diversity, possibly inner neritic because of the relatively common occurrence of *Vesperopsis* and other ceratiacean cysts (e.g., Nøhr-Hansen et al., 2016, table 1). Samples from the Walker Island Member proved mostly devoid of dinocysts, but a few (B-41, B-42, B-53, B-54) yielded rare to relatively common specimens of *Vesperopsis* and *Nyktericysta*,

480 which accords with a marginal marine/deltaic setting for the Walker Island Member. Occasional
481 specimens of *Oligosphaeridium* in these samples may be reworked, but the genus is better
482 represented in the top two samples of the member (B-55 and B-56), indicating more consistent
483 marine conditions prior to the deposition of the overlying Christopher Formation.

484 The four samples tentatively identified as belonging to the Rondon Member yielded a total
485 of 32 dinocyst taxa identified to species level (Fig. 4), including several unnamed species, and
486 several other forms that could not be confidently identified. The assemblage is typical of the middle
487 Early Cretaceous, dominated by gonyaulacaleans, including: common and diverse species of
488 *Oligosphaeridium* (Fig. 4a, L–T); ceratioids such as *Pseudoceratium* (Fig. 4b, D–G) and
489 *Vesperopsis* (Fig. 4b, R–T), although the rarity of specimens of *Odontochitina* is notable; and
490 areoligeraceans represented by frequent *Tenua* (as defined by Fensome et al., 2019) (Fig. 4b, K–
491 L, P). Peridinialeans are restricted to sparse specimens of *Palaeoperidinium* (Fig. 4b, A) and
492 *Subtilisphaera* (Fig. 4b, I).
493
494 *4.2. Pollen and spores*
495
496 Numerous and diverse pollen and spores were recovered from the samples (Fig. 5; Suppl.
497 4). Quantitative analyses of pollen and spores are based on a mean count of 277 (± 69 SD, *n*=32)
498 pollen and spores with affinities to obligately terrestrial plants.
499
500 4.2.1. Terrestrial palynoassemblages
501

Terrestrial palynoassemblages preserved in Isachsen Formation samples from Glacier Fiord are dominated by gymnosperm pollen. Pollen attributable to plants belonging to the class Pinopsida represent, on average, 48% (± 11 SD, *n*=32) of the total sporomorph sum. The majority of pollen attributable to the order Pinales are members of the family Pinaceae (bisaccate pollen, *Laricoidites magnus*, and *Cerebropollenites mesozoicus*), which make up 31% (± 13 SD). *Perinopollenites elatoides* and Cupressaceae-Taxaceae (Cupressales), *Classopollis classoides*, and minor abundances of *Araucariacites australis* and *Podocarpidites* represent the remaining 17% of total Pinopsida pollen. Pollen attributable to Pteridospermopsida represent a minor component (mean <1%) represented by *Vitreisporites pallidus*. Pollen attributable to plants belonging to Cycadales or Gingkoales (*Cycadopites, Monosulcites, Chasmatosporites*, and *Entylissa*) represent a mean of 11% ± 6 SD of the total pollen and spore sum of the samples. *Eucommiidites troedssonii* (Gnetopsida, unknown order) and *Ephedripites* (Ephedrales) pollen have a mean relative abundance of <1% of the pollen and spore population.

Important spore-producing plant groups represented in the palynological record of the Isachsen Formation include Filicopsida *incertae sedis* (mean 11% ± 4 SD, *n*=16 taxa), Osmundales (mean 9% ± 4 SD, *n*=5 taxa), Gleicheniales (mean 9% ± 6 SD, *n*=6 taxa), and Schizaeales (mean 3 ± 3 SD, *n*=17 taxa). Spores with affinities to the Marattiales, Polypodiales, Lycopodiales, Selaginellales, and Bryophyta are rare (mean <3%). Non-pollen and spore palynomorphs observed include undifferentiated dinocysts (mean 3% ± 9 SD), acritarchs (*Veryhachium, Micrhystridium*; mean 0.1% ± 0.5 SD), and chlorophytes (*Tasmanites, Pediastrum, Pterospermella*; mean 0.2% ± 0.3 SD). *Sigmopollis* and *Chomotriletes* are grouped as "other NPP" and represent <0.3% of the assemblage. While *Sigmopollis* is often grouped with acritarchs for the purpose of paleoecological analyses, it is a member of the Cyanophyta (cyanobacteria) according to Krutzsch and Pacltová

(1990). *Chomotriletes* is thought to have affinity to the Charophyceae. While collectively non-pollen and spore palynomorphs represent, on average, less than 4% of the assemblage, dinocysts are an important group in the marine Rondon Member where they increase to 42%.

R-mode cluster analysis is used to delineate six sample clusters that are broadly relatable to the lithostratigraphy of the Isachsen Formation (Fig. 6). Samples from the Rondon Member cluster distinctly due to their high relative proportion of dinocysts. Samples from the Paterson Island and Walker Island members do not appear to differ from each other based on palynomorph content (Fig. 6).

Q-mode cluster analysis was used to define four clusters of taxa (A-D; Fig. 6; Suppl. 3), and the botanical affinities and paleoecology of these taxa are discussed in detail in Suppl. 5. The Pinales form cluster A, Cycadales/Gingkoales, Gleichiniales, Osmundales, Filicopsida of uncertain affinity, and algae and protists (*Tasmanites*, *Pediastrum*, *Pterospermella* and undifferentiated dinocysts) form cluster B. Cluster C is composed of Schizaeales, Sphagnopsida, and indetermined pollen and spores. Cluster D is composed of reworked palynomorphs, Polypodiales, Lycopodiales, Selaginellales, Chierolepidaceae, Marrattiales, Caytoniales, Gnetopsida, bryophytes, and acritarchs (Suppl. 4).

4.3.3 Palynostratigraphy

Stratigraphically constrained cluster analysis of the relative abundance of palynomorphs resulted in delineation of four informal palynological zones (CONISS zones 1–4) and two sub-zones (CONISS subzones 4a, b; Fig. 7). The relative abundance of Q-mode clusters are plotted stratigraphically (Figs. 6, 7). The basal sample has a relatively high abundance of Pinales pollen

(~55%), followed up-section by an increase in the proportion of Cupressales pollen (35%), within the lower part of the Paterson Island Member at Glacier Fiord. Cluster D increases at this level as well, reflecting an increase in the proportion of other NPP. At the top of CONISS zone 1 (*n*=7 samples), an acme in Pinales pollen to near 60% occurs. CONISS zone 2 (*n*=2 samples) is characterized by an increase in cluster C, driven mainly by an increase in the proportion of spores with affinity to the Schizaeaceae. Samples of the Rondon Member cluster as distinct in CONISS zone 3 (*n*=5 samples) by an increase in the relative abundance of dinocysts (up to 42%) and acritarchs. The first occurrence of Marrattiales spores is at base of this zone. CONISS zone 4 comprises samples prepared from the Walker Island Member. CONISS sub-zone 4a (*n*=8 samples) is characterized by an increase in Pinales pollen (up to ~40%), followed by an increase in Cupressales pollen (up to ~30%) and Gleicheniales spores (~30%). The sub-zone is terminated by another increase in Pinales pollen. An acme in Cupressales pollen (~40%) and reworked Paleozoic palynomorphs (up to 3.6%) characterize the base of CONISS sub-zone 4b (*n*=10 samples). This signature is followed by an increase in Pinales pollen before a decline toward the top of the succession where Gleicheniales and then Filicopsida *incertae sedis* peak near the transition to a marginal marine depositional setting. These increases are concurrent with an increase in Marrattiales spores (up to 3%).

5.0 Discussion

5.1. Age interpretation

570 Table 2 indicates some of the more notable ranges (or last or first occurrences) among the
571 dinocyst taxa identified in the Rondon Member of the Glacier Fiord section. Most accord with a
572 Barremian to early Aptian age. The presence of *Muderongia crucis* (Fig. 4a, I–J), considered to
573 have a last occurrence in the early Barremian (e.g. Costa and Davey, 1992; Stover et al. 1996),
574 does not fit with a late Barremian or early Aptian age for the Rondon Member (see below).
575 However, specimens of *Muderongia crucis* in the present material tend to be poorly preserved and
576 thus may be reworked.

577 Dinocysts from the Isachsen Formation in general, and the Rondon Member in particular,
578 have been interpreted previously as indicating a late Barremian age (Costa, 1984; McIntyre, 1984;
579 McIntyre pers. comm. 1984 in Embry, 1985, 1991; Nøhr-Hansen and McIntyre, 1998; Suppl. 1),
580 and based on dinocyst assemblages alone this conclusion remains reasonable. However, the study
581 by Herrle et al. (2015) and Dummann et al. (2021) provided strong evidence that the Rondon
582 Member is of early Aptian age, at least at the Glacier Fiord locality. Hence, it is useful to revisit
583 the dinocyst evidence with the view that the Rondon Member could be younger than Barremian.

584 It can be noted initially that age control of the Lower Cretaceous of the Canadian Arctic
585 based on dinocysts is not as consolidated as in some other regions, such as western Europe; and
586 that ranges, although generally consistent within a region, can be variable from region to region.
587 A key species in assessing the age of the Rondon Member is *Pseudoceratium pelliferum*, which is
588 present in significant numbers in two of the samples (B-36 and B-37) examined in the present
589 study. Both Costa and Davey (1992) and Brinkhuis et al. (2009) considered this species to have a
590 last occurrence in the late Barremian; but according to Stover et al. (1996), the last occurrence of
591 *Pseudoceratium pelliferum* is early Aptian. Another key species is *Pseudoceratium nudum* (also
592 known as *Odontochitina nuda*): Nøhr-Hansen and McIntyre (1998) noted that "The last occurrence

593 of *Pseudoceratium nudum* has previously been recorded as Barremian by Brideaux (1977) but the
594 species appears to range into the early Aptian in East Greenland (Nøhr-Hansen, 1993)." Many of
595 the species encountered in the present study range from the Barremian or older into post-Barremian
596 strata — for example *Chlamydophorella trabeculosa*, *Kiokansium unituberculatum*,
597 *Oligosphaeridium albertense*, *Palaeoperidinium cretaceum*, *Subtilisphaera senegalense*, and
598 *Tenua scabrosa* (which incorporates *Circulodinium asperum* of earlier authors — see Fensome et
599 al., 2019). Although the full age ranges of *Nyktericysta vitrea* and *Vesperopsis mayii*, both found
600 in the Rondon Member in the present study, span beyond the early Aptian, the protologues of both
601 species indicate that their types are from the early Aptian. The first occurrence of
602 *Kleithriasphaeridium cooksoniae* is given as early Aptian in Stover et al. (1996); although only a
603 single specimen was found in the present study, it may add evidence to the possibility that the
604 Rondon Member could be of Aptian age. However, Nøhr- Hansen (1993) recorded similar forms
605 (as *Florentinia cooksoniae* / *Florentinia mantellii*) from the Barremian of North East Greenland.
606 In conclusion with regard to the age of the Rondon Member, dinocysts confirm a late
607 Barremian to early Aptian age, and in conjunction with the carbon isotope data, reasonably
608 conform to an early Aptian age.
609 Pollen and spores preserved in the Isachsen Formation provide less precise age control than
610 the dinocysts and the previously published carbon isotope stratigraphy of Herrle et al. (2015).
611 Pollen and spores are broadly representative of the Early Cretaceous *Cerebropollenites* Province
612 of the northern hemisphere (Herngreen et al., 1996) and are generally similar to an assemblage
613 described from the Isachsen Formation on Ellef Ringnes Island in the central Sverdrup Basin
614 (Galloway et al., 2015). Long-ranging pollen and spore types that characterize the
615 *Cerebropollenites* Province (e.g., *Gleicheniidites*, *Cicatricosisporites*, *Araucariacites*,

616 *Inaperturopollenites*, *Perinopollenites*, *Classopollis*, and *Cerebropollenites mesozoicus*) are
617 unhelpful in providing a more precise age than Early Cretaceous. Many taxa found in the province
618 are common to Late Jurassic floras (Herngreen et al., 1996), with the addition of certain taxa (e.g.,
619 *Aequitriradites*, *Cicatricosisporites*, *Ruffordiaspora*, *Trilobosporites*, and *Foveosporites*
620 *subtriangularis*) that are indicative of a Cretaceous age (Venkatachala and Kar, 1970; Hopkins,
621 1971; Bose and Banerji, 1984; Taugourdeau-Lantz, 1988). *Foveosporites subtriangularis* has been
622 interpreted as an index species for the Hauterivian to late Aptian interval in the eastern North
623 Atlantic (Taugourdeau-Lantz, 1988), and the first occurrence of this spore is in sample B-44 of the
624 Walker Island Member.

625 The preserved palynoassemblages of the Rondon Member cluster distinctly in the NMDS
626 plot due to their high relative abundance of dinocysts (Fig. 6). The palynoassemblages of the
627 Paterson Island Member and the Walker Island Member are similar to each other, with almost 50%
628 of the pollen sum represented by pollen with affinities to the Pinales (Fig. 6). The only notable
629 difference between the terrestrial palynoflora preserved in these two sandstone-dominated units is
630 the occurrence of *Punctatosporites scabratus* (Marrattiales) in the Rondon and Walker Island
631 members and its absence from the Paterson Island Member. This taxon first occurs in the Rondon
632 Member (B-35), above which it remains present in low quantities (up to ~3%). *Punctatosporites*
633 *scabratus* ranges from Late Triassic to late Albian in North America (Singh, 1971 and references
634 therein) and so does not provide useful biostratigraphic information in the present context. This
635 taxon was documented in Upper Triassic rocks in the Canadian Arctic Islands by McGregor
636 (1965).

637

638 *5.2 Vegetation and climate change: the influence of the HALIP*

The Isachsen Formation at Glacier Fiord was deposited over approximately 17 million years, from the base of the Hauterivian to the late Aptian, contemporaneous with the onset of igneous activity associated with the HALIP and tectonism related to the opening of the Amerasia Basin (Figs. 2, 8). The HALIP in the Canadian Arctic was mostly intrusive but volcanic activity of the HALIP is represented by numerous flows in the Isachsen Formation. Vegetation and climate change are explored through analysis of stratigraphic changes in palynoassemblages defined by Q-mode cluster analysis and the potential impacts of the HALIP on climate and terrestrial ecosystems at Glacier Fiord are explored below, and summarized in Figure 8.

5.2.1 Hauterivian–early Barremian warming

The hinterland palynological assemblage (cluster A) is predominant in the lower part of the Paterson Island Member that was deposited during the Hauterivian and early Barremian at Glacier Fiord (CONISS zone 1; Fig. 7). Relatively arid and warm conditions at this time would have supported upland coniferous forests dominated by the Pinaceae (Suppl. 5). On Ellef Ringnes Island, in the underlying Valanginian part of the Paterson Island Member, the abundance of bisaccate pollen are relatively low (~30–40%; Galloway et al., 2015), reflecting the cool climatic conditions that prevailed in high northern latitudes at that time (Price and Nunn, 2010; Vickers et al., 2019). By the Hauterivian, bisaccate pollen had increased to 50–60% of the assemblage on Ellef Ringnes Island, similar to the median abundances of 45% (range 14–55%) of bisaccate pollen in CONISS zone 1 at Glacier Fiord. Galloway et al. (2015) interpreted the increase in bisaccate pollen in the Hauterivian on Ellef Ringnes Island as a response to the development of warmer

climatic conditions. Warming in the Hauterivian following the Valanginian cold interval is widely documented in the northern hemisphere. For example, Gröcke et al. (2005) examined the ^{13}C isotopic signature in fossil plant material from southern Ukraine and showed that the late Valanginian cold phase was short lived (<3 myr), and that the carbon isotope signature of terrestrial plant material had returned to pre-Valanginian levels by the late early Hauterivian. A stable isotope record from belemnites preserved in strata from the Speeton area, eastern England, documents a sea-water warming event from 11°C at the start of the Hauterivian to a maximum of 15°C by middle Hauterivian, before a long-term cooling to 11°C by the start of the Barremian (McArthur et al., 2004). Pucéat et al. (2003) used oxygen isotopes preserved in fish-tooth enamel to quantitatively reconstruct paleotemperatures of upper waters from the western Tethyan platform during the same interval. They show an increase from an early late Valanginian minimum of ~13–14°C to ~20°C during the middle Hauterivian to early Barremian; this was followed by a decline to ~16.5°C from the middle or late Barremian to the earliest Aptian. Podlaha et al. (1998) also showed a general warming trend from the Hauterivian into the Barremian. These data provide evidence of a widespread cooling phase in the northern hemisphere that culminated in the Valanginian, and possibly extended into the early Hauterivian. This cooling event was followed by warming throughout the middle and late Hauterivian and into the Barremian (e.g., Kessels et al., 2006; Price et al., 2018) (Fig. 8).

Valanginian cooling was associated with a widespread positive carbon isotope excursion (the Weissert Event; Erba et al., 2004) in marine sediments, and is dated as 135.22 ± 1 Ma based on U-Pb ages of tuff layers in the Neuquén Basin and an update of the astrochronological time scale of Martinez et al. (2015) (Aguirre-Urreta et al., 2015). The Valanginian "Weissert" event has now been also documented in the Canadian Arctic (Galloway et al., 2019) and North East

Greenland (Möller et al., 2015). This event was associated with a biogeochemical sequence that ultimately led to an increase in carbon burial (Price et al., 2018). An increase in atmospheric CO_2 and environmental changes at this time have been linked to volcanism associated with the Paraná-Etendeka igneous province (e.g., Lini et al., 1992; Gröcke et al. 2005; Erba et al., 2004; Charbonnier et al., 2017), which became active between 134.6 ± 0.6 Ma and 134.4 ± 0.8 Ma; Thiede and Vasconcelos, 2010; Janasi et al., 2001) or slightly earlier, during Chron 15, and remained active for at least 4 myr (Dodd et al., 2015). Rocha et al. (2020) present younger ages for siliciclastic rocks of the Paraná magmatic province (of 133.6 Ma and 132.9 Ma) and thus suggest that magmatism did not trigger the Valanginian event but may have extended its duration. Regardless of the proximal trigger, following the positive carbon isotope excursion of the Weissert Event, the enhanced carbon burial may have triggered a decline in pCO_2, ultimately leading to the cold conditions near the end of the Weissert Event. Price et al. (2018) argued that Paraná-Etendeka volcanism-related global warming did not stimulate the primary productivity that ultimately led to increased carbon burial. They considered instead that the increase in productivity was triggered by ocean fertilization associated with prolonged weathering of basalt. Additionally, they viewed the temperature increase that followed the Paraná–Etendeka episode and the Weissert Event in the Hauterivian as recovery to pre-Weissert event levels (Price et al., 2018) and not an interval of warming forced by volcanic outgassing and CO_2 production. In the Sverdrup Basin, the onset of the HALIP (the oldest age of 126.6 ± 1.2 Ma from a gabbroic intrustion on Ellef Ringnes Island; Evenchick et al., 2015) was initiated possibly as early as the latest Hauterivian or earliest Barremian, and thus post-dates the Hauterivian warming interval.

5.2.2 Volcanic flows and a “fern spike”

By the middle to late Barremian, the hinterland assemblage at Glacier Fiord had declined and was replaced by a mixed heathland and mire assemblage (Q-mode cluster C) marked by an increase in fern spores up to 70% of the assemblage in the uppermost Paterson Island Member. This brief vegetation change can be considered coeval with the first pulse of the HALIP, that, with error, spans from 127.8 Ma to 120 Ma (Figs. 7, 8). Schizaeales and Gleicheniales each represent ~20% of the total assemblage. The uppermost Paterson Island Member is a transgressive unit deposited during relative sea-level rise that culminated in the maximum flood that deposited the overlying marine Rondon Member. This eliminates sea-level fall that would have exposed delta plains to be colonized by early successional vegetation as the proximate driver of the spore spike. The increase of filicopsid spores in the floodplain deposits of the uppermost Paterson Island Member during the middle to late Barremian could reflect an increase in humidity and disturbance at this time that drove the expansion of mire and heathland plant communities. A small increase in other NPP (*Sigmopollis* and *Chomotriletes*; Fig. 8) indicate the presence of wet biotopes and standing water during this interval (Suppl. 5). Increased effective moisture at this time may have been related to the overall cooling climate conditions that began during the late Barremian and progressed into the Aptian (Pucéat et al., 2003). Relative sea-level rise at this time could have also decreased depth to water table in the broader environment, leading to wetter soils and more frequent and severe flooding. However, while filicopsid spores can range up to 70–75% in coal samples deposited in humid environments during the Jurassic and Cretaceous in the mid-latitudes of the southern hemisphere (Schrank, 2010, and references therein), values near 30–40% are typical for the Isachsen Formation (this work; Galloway et al., 2015).

730 Environmental change can also cause conversion of temperate forests into heaths due to
731 disturbance-mediated increases in paludification, nutrient sequestration, release of allelochemicals
732 and contaminants, and soil acidification that cause conifer regeneration failure (Mallik, 1995). The
733 dominance of ferns following disturbance is the result of their tolerance of ecological stress,
734 including the ability to grow on strongly leached and/or nutrient poor or metal-enriched soils, their
735 tolerance of low-light conditions, and certain life-cycle traits such as gametophytic selfing and
736 wind dispersal of spores; together these traits permit their rapid invasion of and growth in disturbed
737 habitats (Page, 2002).

738 Fern spore spikes are commonly documented in the geological record associated with
739 large-scale disturbance, including those related to LIP magmatism. Crises at the end-Permian (e.g.,
740 Hochuli et al., 2010), end-Triassic (e.g., van de Schootbrugge et al., 2009 and references therein),
741 and end-Cretaceous (e.g., Vajda and Bercovici et al., 2014 and references therein) demonstrate
742 similar successions of recovery phases of terrestrial vegetation, characterized by a bloom of
743 opportunistic taxa followed by a pulse of pioneer communities and finally recovery of plant
744 communities (Vajda and Bercovici, 2014). Ferns are the most common pioneer taxa, although
745 bryophyte spores may also provide this signal (Brinkhuis and Schiøler, 1996). Geologically brief
746 fern spikes are interpreted to represent the pioneering recovery stage by ferns and fern-allies
747 following collapse of arboreal communities associated with widespread disturbance (e.g., van de
748 Schootbrugge et al., 2009). For example, at the end-Cretaceous extinction event, a dramatic
749 increase in the percentage of fern spores is documented in assemblages immediately overlying the
750 iridium anomaly (e.g., Tschudy et al., 1984; Tschudy and Tschudy, 1986; Nichols et al., 1986).
751 Berry (2019) noted that following the Cretaceous/Paleogene boundary, post-extinction recovery
752 flora was dominated by *Cyathidites* and then *Laevigatosporites* fern spores. Schizaeaceae are also

notable early pioneers of disturbed habitats; for example, this group were the first plants to colonize a barren landscape following a volcanic eruption that preserved the Eocene Lagerstätte in Messel, Germany (Lenz et al., 2007). The magnitude of the fern-spore spike appears related to the severity of the crises; across the Cretaceous/Paleogene boundary, an increase in fern spores to ~70–100% (cf. 70% abundance in Isachsen Formation samples) of the total pollen and spore assemblage occurred (Vajda and Bercovici, 2014 and references therein). The Cretaceous/Paleogene fern spore spike was geologically brief, recorded in only a 1–2 cm-thick interval (Vajda and Bercovici, 2014).

Magmatism can be the agent of environmental disturbance provoking vegetation change, and basalt flows are abundant in the Paterson Island Member. Lava flows destroy vegetation in their immediate path and can cause widespread wildfire (e.g., van de Schootbrugge et al., 2009). For example, charcoal records from Greenland, Denmark, Sweden, and Poland show increased wildfire activity (leading to further CO_2 release) associated with emplacement of the Central Atlantic Magmatic Province (CAMP; Lindström et al., 2015). Grasby et al. (2011) documented fly-ash generated from coal combustion during the Siberian Trap LIP emplacement. In Triassic-Jurassic strata of the Newark Supergroup of eastern North America affected by CAMP volcanism, palynological assemblages change to a higher abundance of trilete spores occurs approximately 10 m below (and ~10 kyr prior) to the first exposed flood basalt flows of the Newark Supergroup (Fowell and Olsen, 1993). In northwestern Europe, an increase in Schizaeaceae spores (up to 35%) and Osmundaceae spores (up to 5–10%) occur in uppermost Triassic Triletes beds in response to magmatism associated with the CAMP (van de Schootbrugge et al., 2009). The dominance of pteridophyte vegetation across more than 2000 km^2 within Triassic/Jurassic boundary beds indicates that this floral change was unlikely to be due to a major sea-level fall that would have promoted growth of riparian habitats (van de Schootbrugge et al., 2009). Fern spikes are also well

776 documented in response to smaller scale disturbances. For example, ferns were early colonizers of
777 denuded ground after landslides associated with 1980 Mount St. Helens eruption, and were
778 dominant plants following the 1883 Krakatau eruption (Tschudy et al., 1984), and are the first
779 colonizers of freshly deposited lava flows in Hawaii (Bercovici and Vellekoop, 2017 and
780 references therein).

781 In the Glacier Fiord assemblage, the increase in spore abundance from 30–40% to ~70%
782 of the total palynoassemblage in the uppermost 20 m of the Paterson Island Member may reflect a
783 response to landscape disturbance associated with the first volcanic flows of the HALIP in the
784 Sverdrup Basin, or their geologically brief occurrence may be a coincidence or due to other factors
785 such as disturbance or rising sea-level (Fig. 8). The basalts preserved in the Isachsen Formation
786 indicate widespread volcanism that was likely to have impacted polar vegetation through, for
787 example: i) release of sulfur aerosols and resulting short-term cooling and inhibition of
788 photosynthesis triggered by darkening; ii) decrease in stratospheric ozone as a result of release of
789 brominated and chlorinated halocarbons from heated evaporites and resulting increase in lethal
790 radiation (but insufficient to cause aberrant spores); iii) acid rain; and/or iv) direct toxic effects
791 from the release of polycyclic aromatic hydrocarbons and mercury (e.g., Svensen et al., 2009;
792 Lindström et al., 2019). The direct impact of these effects are not evaluated here, although we note
793 that no aberrant pollen or spores were documented (cf. Lindström et al., 2019). However, because
794 ferns are common early colonizers following localized landscape disturbances associated with
795 scoured riverbanks, dunes, and floodplains (Walker and Sharpe, 2010 and references therein),
796 multiple studies across a wide geographical area are needed to test the hypothesis that the spore
797 spike was caused by HALIP-related landscape disturbance, atmospheric toxicity (e.g., van de
798 Schootbrugge et al., 2009), sea-level change, or is a coincidence.

799

800 5.3.3 Ocean Anoxic Event 1a

801

802 Palynoassemblages preserved in the marine Rondon Member are dominated by dinocysts
803 (up to ~40%; Figs. 7, 8). Ocean Anoxic Event 1a (~121–122 Ma; Midtkandal et al., 2016; Olierook
804 et al., 2019) is recorded as a major negative carbon isotope excursion in the marine mudstones of
805 this unit at Glacier Fiord (Herrle et al., 2015).

806 In the Tethys, warmer temperatures are inferred to have developed and culminated in a
807 maximum sea-surface temperature during the early onset of the negative carbon isotope excursion
808 associated with OAE 1a (Hu et al., 2012; Bottini et al., 2015; Naafs and Pancost, 2016; Jenkyns,
809 2018). This warming is thought to be the result of intense volcanic activity of the Ontong-Java
810 Plateau (Wang et al., 2014; Bottini et al., 2015; Adloff et al., 2020) In the Boreal Realm, sea-
811 surface temperature rose prior to OAE 1a and reached a maximum of 4–9 ° C higher than
812 temperatures recorded for Hauterivian–lowermost Aptian sediments from the same basin, showing
813 that "supergreenhouse" conditions existed even at paleolatitudes of up to 39 ° N (northwestern
814 Germany; Mutterlose et al., 2014). This magnitude of warming is comparable to that experienced
815 during the end-Triassic event (~3–4°C; McElwain et al., 1999) that was associated with
816 emplacement of ~700,000 km^3 of sills during the Central Atlantic Magmatic Event (Svensen et al.,
817 2017) that could have produced up to 88,000 Gt CO_2 through contact metamorphism of organic-
818 rich shales and hydrocarbon reservoirs (Svensen et al., 2017). The end of the Aptian OAE 1a
819 coincided with cessation of Ontong-Java Plateau volcanics and pronounced cooling in the
820 Vocontian Basin (Herrle et al., 2010; Kuhnt et al., 2011), Boreal Realm (Rückheim et al., 2006;
821 Malkoč et al., 2010; Bottini and Mutterlose, 2012; Pauly et al., 2013; Mutterlose and Bottini, 2013;

822 Mutterlose et al., 2014) and Pacific Ocean (Jenkyns, 1995; Jenkyns and Wilson, 1999; Price, 2003;
823 Dumitrescu et al., 2006; Ando et al., 2008).

824 Because of the broad temporal coincidence of the onset of OAE 1a with the emplacement
825 of Ontong-Java Plateau, the negative carbon isotope excursion has been interpreted as resulting
826 from a stepwise accumulation of volcanogenic CO_2 and release of isotopically light carbon from
827 partial methane hydrate dissociation, and initiating OAE 1a by warming of the climate and
828 nutrification of the ocean (e.g., Weissert, 1989; Jahren et al., 2001). Using a similar argument, the
829 temporal coincidence of the HALIP with OAE 1a also suggests that this high latitude LIP could
830 have played a role in carbon cycle and climate perturbations at this time (Polteau et al., 2016;
831 Planke et al., 2017; Adloff et al., 2020). For example, the volume of igneous rocks associated with
832 the Barents Sea Sill Complex of the northern and eastern Barents Sea (a conservative volume
833 estimate of 100,000 to 200,000 km^2 of intrusions in an area of an area of ~900,000 km^2), that
834 intruded mostly into Triassic and Permian sedimentary rocks resulted in thermogenic gas
835 formation and mobilization of up to 20,000 Gt of carbon and may have triggered OAE 1a and the
836 associated carbon isotope excursion in the early Aptian (Polteau et al., 2016; Planke et al., 2017;
837 Adloff et al., 2020). The age of magma emplacement is interpreted as ~125–122 Ma (Barremian;
838 Tarduno et al., 1998; Corfu et al., 2013; Polteau et al., 2016). Although ages of sills in the Sverdrup
839 Basin are poorly constrained, abundant sills of probably the same age as the Barents sills, intrude
840 into uppermost Permian and Triassic source rocks of the Blind Fiord, Murray Harbour, Hoyle, and
841 Barrow formations (e.g., Hadlari et al., 2018). The earliest well-dated intrusive components of the
842 HALIP were emplaced into the Upper Jurassic Deer Bay Formation and the Isachsen Formation
843 on Ellef Ringnes Island at 127 Ma and 121 Ma (Evenchick et al., 2015; Fig. 2). The HALIP is by
844 volume at least 3–5 times more intrusive than extrusive in character in its Canadian part, and

possibly 50–60% of the HALIP rock mass occurs as sills (Saumur et al., 2016). The total volume of magma in Canada alone is estimated as exceeding 100,000 km^3 (Saumur et al., 2016). The magmatic rocks associated with the HALIP exposed on Svalbard also occur mostly as sills (Maher, 2001; Senger et al., 2014 and references therein). It is primarily the intrusive magmatism associated with LIPs that generates volatiles and releases CO_2 through interaction with host rocks rich in organic matter and/or evaporites (e.g., Jones et al., 2016; Heimdal et al., 2018). Interaction of the early igneous events associated with the HALIP with organic-rich rocks of the Sverdrup Basin and other intruded northern basins would have released greenhouse gases into the atmosphere during the early Aptian.

The low sampling resolution of the Rondon Member for palynology at the Glacier Fiord section does not permit comparison of sequence of OAE 1a initiation and vegetation change. In better studied and expanded sections in lower latitudes, palynological and $\delta^{18}O$ records of a contemporaneous section in the Lombardian and Belluno basins, Italy (Keller et al., 2011), and the shelf section at La Bédoule, SE France (Lorenzen et al., 2013) show a time lag between the start of the negative carbon isotope excursion associated with OAE 1a and the main interval of warming. This lag is consistent with reconstructions by Adloff et al. (2020) that show that *p*CO2 increased, the driver of the climate warming and subsequent activation of the hydrological cycle causing increased nutrient flux to global oceans due to higher weathering rates (Jenkyns, 2010), after the onset of the carbon isotope excursion caused by release of a ^{13}C-depleted carbon source. Keller et al. (2011) show that during the C3 interval (onset of the CIE; *sensu* Menegatti et al., 1998) in the Lombardian and Belluno basins, an increase in *Classopollis* pollen occurred, with peak values in the lower C4 segment. The upper part of C4 and the C5 and C6 segments are marked by high but fluctuating *Classopollis* pollen abundance, followed by a decline subsequent to the termination of

868 the black shale episode. In the Belluno Basin, the decline in *Classopollis* pollen is paralleled by an
869 increase in post-OAE bisaccate pollen abundance, interpreted to reflect cooling and an increase in
870 humidity that followed OAE 1a (Hochuli et al., 1999). In the Maestrat Basin of eastern Spain, Cors
871 et al. (2015) showed the climate cooling that appears to punctuate OAE 1a (e.g., Jenkyns, 2018) is
872 also manifested as changes in terrestrial vegetation after the end of carbon drawdown. The climatic
873 cooling triggered initially by carbon drawdown and deposition and preservation of marine black
874 shales may have resulted in the equator-wards expansion of temperate humid belts, and resulting
875 in the expansion of peat-forming environments that persisted after OAE 1a (McCabe and Parrish,
876 1992; Cors et al., 2015); thus OAE 1a left a legacy of prolonged change from predominantly
877 marine to terrestrial carbon burial on a large scale. This protracted phase of terrestrial carbon burial
878 in the aftermath of OAE 1a may partially explain the interval characterized by positive carbon
879 isotope values during late early Aptian time (Cors et al., 2015), and possibly partially the floral
880 instability that ensued in the early Aptian at Glacier Fiord.
881
882 5.3.4 Early Aptian floral instability
883
884 The early Aptian at Glacier Fiord is characterized by fluctuations in Pinaceae pollen and
885 Cupressales pollen and fern spores (Figs. 7, 8). Two declines in the abundance of Pinaceae pollen
886 in fluvial to shoreface deposits of the lower Walker Island Member and shoreline to shallow marine
887 deposits of the upper Walker Island Member are notable. These declines are associated with
888 increases in Cupressales pollen and fern spores. Floral changes between dominance of Pinaceae
889 vs. Cupressales and ferns at Glacier Fiord likely reflect a combination of climate change associated
890 with long-term instability following OAE 1a, landscape disturbance associated with relative sea-

level rise that would have destabilized lowland coastal environments, and/or lava flows associated with the HALIP that were repeatedly extruded onto the subsiding delta plain on Axel Heiberg Island during deposition of the Walker Island Member (Emby and Osadetz, 1988). Volcanic activity in the early Aptian is likely to have affected the landscapes of southern Glacier Fiord, resulting in repeated perturbation of gymnosperm-dominated forests and replacement by earlier successional communities dominated by Cupressales and ferns.

5.0 Conclusions

Large Igneous Provinces are increasingly accepted to have caused major global shifts in environmental conditions, and to be implicated in mass extinctions and smaller scale biotic crises (e.g., Ernst and Youbi, 2017, and references therein). The proximal causal mechanisms of environmental change associated with LIPs are global warming and cooling, ocean anoxic events, ocean acidification, introduction of toxic metals and gases, removal of bio-essential elements, and sea-level change (summarized in Ernst and Youbi, 2017). The absence of a relationship between LIP size and magnitude of extinction demonstrates complexities. The duration of short-term pulses of activity, extending down to the scale of individual flows, is probably more important than the overall volume of the event. LIPs are associated with some of the largest volcanic episodes in Earth's history, including areally extensive basaltic lava-flow fields. Lava flows destroy vegetation in their immediate path and cause widespread wildfire (e.g., van de Schootbrugge et al., 2009). Other environmental effects related to LIPs may be the rapid thermal maturation of organic-rich sediments that igneous bodies contact, and the associated volitolization of gases contained in those sediments. The gas thus released is composed dominantly of H_2O, but also of CO_2, SO_2 and

914 halogens (e.g., Self et al., 2014). The release of SO_2 can lead to warming and then cooling (when
915 converted to sulphuric acid and then to sulphate aerosols). Ozone-destroying halogens may also
916 be released via the intrusive component of LIPs interaction with volatile-rich sediments (Svensen
917 et al., 2009). Mercury can also be released, with deleterious environmental effects (Sanei et al.,
918 2012), including on vegetation (Lindström et al., 2019). A myriad of these effects commonly
919 associated with LIPs, coupled with landscape disturbance that may have been associated with the
920 fluvial and deltaic depositional setting of the Isachsen Formation and influenced Arctic vegetation
921 during the Hauterivian to Aptian interval in the Sverdrup Basin. The interval of Hauterivian to
922 early Barremian warming preserved in floral assemblage change from Glacier Fiord in Arctic
923 Canada may be related to recovery from the Valanginian cold snap and/or CO_2 forced warming
924 associated with LIP activity in mid and low latitudes (Paraná-Etendeka Province). An increase in
925 fern spores up to 70%, comparable in abundance to spore spikes associated with mass extinctions
926 (e.g., latest Permian, latest Triassic), in the uppermost Paterson Island is herein interpreted as a
927 possible floral response to the initial flood basalt activity of the HALIP that disturbed landscapes
928 in the proximity of Glacier Fiord. OAE 1a, documented at Glacier Fiord by a carbon isotope
929 excursion in the marine Rondon Member, was probably at least partially triggered by CO_2
930 outgassing associated with contact metamorphism of intrusive components of the HALIP with
931 carbon-rich rocks. Lastly, floral instability preserved as fluctuations in the proportion of pollen
932 from trees in the hinterland during deposition of the Walker Island Member in the early Aptian is
933 interpreted as a possible response to temperature instability following OAE 1a and repeated lava
934 flows of the HALIP onto the subsiding delta plain on southern Axel Heiberg Island that disturbed
935 vegetation and habitats. This analysis of the palynological signature of the Isachsen Formation
936 exposed in the eastern Sverdrup Basin at Glacier Fiord refines the understanding of drivers of

Arctic climate change during Hauterivian to Aptian time by illustrating the effects of the HALIP on at least regional climate and habitat that, in turn, affected Arctic forest composition.

Acknowledgements

Financial support was provided by the GeoMapping for Energy and Minerals (GEM) Program (Natural Resources Canada, Geological Survey of Canada), an NSERC Visiting Fellowship in a Canadian Government Laboratory (JMG) and the AIAS-COFUND II fellowship programme that was supported by the Marie Skłodowska-Curie actions under the European Union's Horizon 2020 (Grant agreement no. 754513) and the Aarhus University Research Foundation (JMG). We are grateful to Keith Dewing for project management. We thank Ashton Embry for directing us to study the Glacier Fiord section and for sharing his extensive knowledge on the Svedrup Basin, the Isachsen Formation, and the Glacier Fiord section in particular with us. We thank him for spending time with us on the section during our field season in 2011. We acknowledge the logistics support provided by the Polar Continental Shelf Program (pilot Massimo Zancolò). Linda Dancey (GSC) is thanked for palynological preparation and Richard Fontaine for curation. RAF would like to thank Andrew MacRae and Graham Williams of Saint Mary's University and GSC Atlantic, respectively for a discussion on aspects of the dinocyst assemblage. This publication represents NRCan Contribution Number/Numéro de contribution de RNCan (pending). We are grateful for the comments and suggestions of Manuel Bringué (Geological Survey of Canada) for his interval review. We thank Henrik Nøhr-Hansen and two anonymous reviewers for providing constructive and helpful comments that improved this manuscript.

960 **Literature Cited**

961

962 Adloff, M., Greene, S.E., Parkinson, I.J., Naafs, B.D.A., Preston, W., Ridgwell, A., Lunt, D.J.,
963 Manuel, J., Jiménez, C., Monteiro, F.M., 2020. Unravelling the sources of carbon emissions at the
964 onset of Oceanic Anoxic Event (OAE) 1a. Earth and Planetary Science Letters 530, 115947.

965

966 Aguirre-Urreta, B., Lescano, M., Schmitz, M. D., Tunik, M., Concheyro, A., Rawson, P. F.,
967 Ramos, V. A., 2015. Filling the gap: new precise Early Cretaceous radioisotopic ages from the
968 Andes. Geological Magazine 152, 557–564.

969

970 Alberti, G., 1961. Zur Kenntnis mesozoischer und alttertiärer Dinoflagellaten und
971 Hystrichosphaerideen von Nord- und Mitteldeutschland sowie einigen anderen europäischen
972 Gebieten (Knowledge of Mesozoic and old Tertiary dinoflagellates and Hystrichosphaerideen
973 from northern and central Germany as well as some other European areas). Palaeontographica
974 Abteilung A 116, 1–58, pl.1–2.

975

976 Ando, A., Kaiho, K., Kawahata, H., Kakegawa, T., 2008. Timing and magnitude of early Aptian
977 extreme warming: unraveling primary delta ^{18}O variation in indurated pelagic carbonates at Deep
978 Sea Drilling Project Site 463, central Pacific Ocean. Palaeogeography, Palaeoclimatology,
979 Palaeoecology 260, 463–476.

980

Anfinson, O.A., Embry, A.F., Stockli, D.F., 2016. Geochronologic constraints on the Permian–Triassic northern source region of the Sverdrup Basin, Canadian Arctic Islands. Tectonophysics 691, 206–219.

Archangelsky, S., Gamerro, J.C., 1966. Estudio palinológico de la formación Baqueró (Cretácico), Provincia de Santa Cruz. II. (Palynological studies of the Baquero Formation (Cretaceous), Santa Cruz Province, Argentina. II). Ameghiniana 4, 201–209.

Balkwill, H. R., 1978. Evolution of Sverdrup Basin, Arctic Canada. American Association of Petroleum Geologists, Bulletin 62, 1004–1028.

Balkwill, H.R., Hopkins, W.S. Jr., Wall, J.H., 1982. Geology, Lougheed Island, District of Franklin. Geological Survey of Canada, Memoir 395, 22 p. (3 sheets).

Balme, B.E., 1957. Spores and pollen grains from the Mesozoic of Western Australia. Commonwealth Scientific and Industrial Research Organization (Australia), Coal Research Section, Reference T.C.25, 1–48, pl.1–11.

Bambach, R. K., Bennington, J.B., 1996. Do communities evolve? A major question in evolutionary paleoecology. In: Jablonski, D., Erwin, D.H., Lipps, J. (eds.), Evolutionary paleobiology: essays in honor of James W. Valentine, University of Chicago Press, Chicago, 123–160.

Batten, D.J. and Lister, J.K., 1988. Early Cretaceous dinoflagellate cysts and chlorococcalean algae from freshwater and low salinity palynofacies in the English Wealden. Cretaceous Research 9, 337–367.

Bédard, J., Troll, V., Deegan, F., 2016. HALIP intrusions, contact metamorphism, and incipient diapirism of gypsum–carbonate sequences. In: Williamson, M.-C. (ed.), Report of activities for the High Arctic Large Igneous Province (HALIP)—GEM 2 Western Arctic Region Project: bedrock mapping and mineral exploration. Open File 7950. Geological Survey of Canada, p. 3–13.

Beil, S., Kuhnt, W., Holbourn, A., Scholz, F., Oxmann, J., Wallmann, K., Lorenzen, J., Aquit, M.,Chellai, E. H., 2020, Cretaceous Oceanic Anoxic Events prolonged by phosphorus cycle feedbacks: Climate of the Past 16, 757–582.

Below, R., 1981. Dinoflagellaten-Zysten aus dem oberen Hauterive bis unteren Cenoman Süd-West-Marokkos (Dinoflagellate cysts from the upper Hauterivian to lower Cenomanian in south-west Morocco). Palaeontographica Abteilung B 176, 1–145, pl.1–15.

Benedek, P.N., 1972. Phytoplanktonten aus dem Mittel- und Oberoligozän von Tönisberg (Niederrheingebiet) (Phytoplankton from the middle and upper Oligocene of Tönisberg (lower Rhine region). Palaeontographica Abteilung B 137, 1–71, pl.1–16.

Bennington, J B., Bambach, R.K., 1996. Statistical testing for paleocommunity recurrence: are similar fossil assemblages ever the same? Palaeogeography, Palaeoclimatology, Palaeoecology 127, 107–133.

Bercovici, A., Vellekoop, J., 2017. Methods in paleopalynology and palynostratigraphy: an application to the K–Pg boundary. In: Zeigler, K.E., Parker, W.G. (eds), Terrestrial depositional systems: deciphering complexities through multiple stratigraphic models. Elsevier, Amsterdam, 127–164.

Berry, K., 2019. Linking fern foliage with spores at the K–Pg boundary section in the Sugarite coal zone, New Mexico, USA, while questioning the orthodoxy of the global pattern of plant succession across the K–Pg boundary. Neues Jahrbuch für Geologie und Paläontologie - Abhandlungen (New yearbook for geology and paleontology – treatises) 291, 159–169.

Bice, K.L., Norris, R.D., 2002. Possible atmospheric CO_2 extremes of the middle Cretaceous (late Albian–Turonian). Paleoceanography 17, 1070.

Bint, A.N., 1986. Fossil Ceratiaceae: a restudy and new taxa from the mid-Cretaceous of the Western Interior, U.S.A. Palynology 10, 135–180.

Bolkhovitina, N.A., 1953. Sporovo-pyltsevaya kharakteristika melovykh otlozhenii tsentralnykh oblastei SSSR (Spore-pollen characterization of Cretaceous deposits of the central regions of the USSR). Geologicheskiy Institut, Akademiya Nauk SSSR, Trudy (Geological Institute, Academy of Sciences of the USSR, Proceedings) 145, 184 p., 16 pl.

Bose, M.N., Banerji, J., 1984. The flossil floras of Kachchh. I—Mesozoic megafossils. The Palaeobotanist 33, 1–189.

Bottini, C., Mutterlose, J., 2012. Integrated stratigraphy of early Aptian black shales in the Boreal Realm: calcareous nannofossil and stable isotope evidence for global and regional processes. Newsletters on Stratigraphy 45, 115–137.

Bottini, C., Erba, E., Tiraboschi, D., Jenkyns, H.C., Schouten, S., Sinninghe Damasté, J.S., 2015. Climate variability and ocean fertility during the Aptian Stage. Climate of the Past 11, 383–402.

Boutelier, J., Cruden, A., Brent, T., Stephenson, R., 2010. Timing and mechanisms controlling evaporate diapirism on Ellef Ringnes Island, Canadian Arctic Archipelago. Basin Research 23, 478–498.

Brenner, G.J., 1963. The spores and pollen of the Potomac Group of Maryland. Maryland Department of Geology, Mines and Water Resources, Bulletin 27, 1–215, pl.1–43.

Brideaux, W.W. 1975. Taxonomic note: redefinition of the genus *Broomea* and its relationship to *Batioladinium* gen. nov. (Cretaceous). Canadian Journal of Botany 53, 1239–1243.

1070 Brideaux, W.W., 1977. Taxonomy of Upper Jurassic–Lower Cretaceous microplankton from the
1071 Richardson Mountains, District of Mackenzie, Canada. Geological Survey of Canada, Bulletin
1072 281, 1–89, pl.1–16.
1073
1074 Brinkhuis, H., Schiøler, P., 1996. Palynology of the Geulhemmerberg Cretaceous/Tertiary
1075 boundary section (Limburg, SE Netherlands). Geologie en Mijnbouw 75, 193–213.
1076
1077 Bush, A.M., Balme, R.I., 2010. Multiple paleoecological controls on the composition of marine
1078 fossil assemblages from the Frasnian (Late Devonian) of Virginia, with a comparison of ordination
1079 methods. Paleobiology 36, 573–591.
1080
1081 Charbonnier, G., Morales, C., Duchamp-Alphonse, S., Westermann, S., Adatte, T., Föllmi, K.B.,
1082 2017. Mercury enrichment indicates volcanic triggering of Valanginian environmental change.
1083 Scientific Reports 7, 40808.
1084
1085 Cookson, I.C., 1947. Plant microfossils from the lignites of Kerguelen Archipelago. B.A.N.Z.
1086 Antarctic Research Expedition 1929–1931, Report Series A 2, 127–142, pl.13–17.
1087
1088 Cookson, I.C., 1953. Difference in microspore composition of some samples from a bore at
1089 Comaum, South Australia. Australian Journal of Botany 1, 462–473, pl.1–2.
1090
1091 Cookson, I.C., Dettmann, M.E., 1958. Some trilete spores from upper Mesozoic deposits in the
1092 eastern Australian region. Proceedings of the Royal Society of Victoria 70, 95–128.

Cookson, I.C., Dettmann, M.E., 1961. Reappraisal of the Mesozoic microspore genus *Aequitriradites*. Palaeontology 4, 425–427, pl.52.

Cookson, I.C., Eisenack, A., 1958. Microplankton from Australian and New Guinea upper Mesozoic sediments. Proceedings of the Royal Society of Victoria 70, 19–79, pl.1–12.

Cookson, I.C., Eisenack, A., 1960. Upper Mesozoic microplankton from Australia and New Guinea. Palaeontology 2, 243–261.

Cookson, I.C., Eisenack, A., 1970. Cretaceous microplankton from the Eucla Basin, Western Australia. Proceedings of the Royal Society of Victoria 83, 137–157.

Corfu, F., Polteau, S., Planke, S., Faleide, J.I., Svensen, H., Zayoncheck, A., Stolbov, N., 2013. U–Pb geochronology of Cretaceous magmatism on Svalbard and Franz Josef Land, Barents Sea Large Igneous Province. Geological Magazine 150, 1127–1135.

Cors, J., Heimhofer, U., Adatte, T., Hochuli, P.A., Huck, H., Bover-Arnal, T., 2015. Climatic evolution across Oceanic Anoxic Event 1a derived from terrestrial palynology and clay minerals (Maestrat Basin, Spain). Geological Magazine 154, 632–647.

1114 Costa, L.I., 1984. Dinoflagellate stratigraphy of samples from the Isachsen and Christopher
1115 formations, Arctic Canada. Report prepared for the Geological Survey of Canada (Calgary).
1116 Unpubl., 3 p.
1117
1118 Costa, L.I., Davey, R.J., 1992. 3. Dinoflagellate cysts of the Cretaceous System. In: Powell, A.J.
1119 (ed.), A stratigraphic index of dinoflagellate cysts; British Micropaleontological Society Series,
1120 Chapman & Hall, London, 99–154.
1121
1122 Couper, R.A., 1953. Upper Mesozoic and Cainozoic spores and pollen grains from New Zealand.
1123 New Zealand Geological Survey, Paleontological Bulletin 22, 5–77, pl.9.
1124
1125 Couper, R.A., 1958. British Mesozoic microspores and pollen grains — a systematic and
1126 stratigraphic study. Palaeontographica Abteilung B 103, 75–179, pl.15–31.
1127
1128 Danzé-Corsin, P., Laveine, J.-P., 1963. B. Microflore (Microflora). In: Briche, P., Danzé-Corsin,
1129 P., Laveine, J.-P. (eds.), Flore infraliassique du Boulonais (macro- et microflore) (Boulra infra-
1130 Liassic flora (macro-and microflora). Société géologique du Nord Mémoires (Northern Geolgoical
1131 Society Memoirs) 13, 57–110, pl. 5–11.
1132
1133 Davey, R.J., 1969. Non-calcareous microplankton from the Cenomanian of England, northern
1134 France and North America, part I. British Museum (Natural History) Geology, Bulletin 17, 103–
1135 180, pl.1–11.
1136

Davey, R.J., 1970. Non-calcareous microplankton from the Cenomanian of England, northern France and North America, part II. British Museum (Natural History) Geology Bulletin 18, 333–397, pl. 1–10.

Davey, R.J., 1978. Marine Cretaceous palynology of Site 361, D.S.D.P. Leg 40, off southwestern Africa. In: Bolli, H.M. et al., Deep Sea Drilling Project, Washington, Initial Reports 40, 883–913, pl.1–9.

Davey, R.J., 1982. Dinocyst stratigraphy of the latest Jurassic to Early Cretaceous of the Haldager No. 1 borehole, Denmark. Danmarks Geologiske Undersøgelse (Geolgoical Survey of Denmark), Series B no.6, 1–57, pl.1–10.

Davey, R.J., Williams, G.L., 1966. V. The genus *Hystrichosphaeridium* and its allies. In: Davey, R.J., Downie, C., Sarjeant, W.A.S., Williams, G.L. (eds.), Studies on Mesozoic and Cainozoic dinoflagellate cysts; British Museum (Natural History) Geology, Bulletin, Supplement 3, 53–106.

Davey, R.J., Williams, G.L., 1969. Generic reallocations. In: Davey, R.J., Downie, C., Sarjeant, W.A.S., Williams, G.L. (eds.), Appendix to "Studies on Mesozoic and Cainozoic dinoflagellate cysts"; British Museum (Natural History) Geology Bulletin, Appendix to Supplement 3, 4–7.

Davey, R.J., Verdier, J.-P., 1974. Dinoflagellate cysts from the Aptian type sections at Gargas and La Bédoule, France. Palaeontology 17, 623–653.

Davey, R.J., Downie, C., Sarjeant, W.A.S., Williams, G.L., 1966. VII. Fossil dinoflagellate cysts attributed to *Baltisphaeridium*. In: Davey, R.J., Downie, C., Sarjeant, W.A.S., Williams, G.L. (eds.), Studies on Mesozoic and Cainozoic dinoflagellate cysts; British Museum (Natural History) Geology Bulletin, Supplement 3, 157–175.

Davies, E.H., 1983. The dinoflagellate Oppel-zonation of the Jurassic-Lower Cretaceous sequences in the Sverdrup Basin, Arctic Canada. Geological Survey of Canada, Bulletin 359, 1–59.

Davis, W. J., Schröder-Adams, C., Galloway, J. M., Herrle, J., Pugh, A., 2016. U–Pb geochronology of bentonites from the Upper Cretaceous Kanguk Formation, Sverdrup Basin, Arctic Canada: constraints on sedimentation rates, biostratigraphic correlations and the late magmatic history of the High Arctic Large Igneous Province. Geological Magazine 154, 757–776.

Deflandre, G., 1934. Sur les microfossiles d'origine planctonique, conservés à l'état de matière organique dans les silex de la craie (On planktonic microfossils, preserved as organic matter in chalk flints). Comptes rendus hebdomadaires des séances de l'Académie des sciences (Weekly reports of meetings of the Academy of Sciences) 199, 966–968.

Deflandre, G., 1937. Microfossiles des silex crétacés. Deuxième partie. Flagellés incertae sedis. Hystrichosphaeridés. Sarcodinés. Organismes divers (Cretaceous flint microfossils. Part 2. Flagellated incertae sedis. Hystrichosphaerides. Sarcodines. Various organizations). Annales de paléontologie (Annals of paleontology) 26, 51–103 (al. 3–55), pl.11–18 (al. pl.8–15).

Deflandre, G., 1947. Sur quelques microorganismes planctoniques des silex Jurassiques (On some planktonic microorganisms from Jurassic flints). Institut océanographique, Monaco, Bulletin (Oceanographic onstitute, Monaco, Bulletin) 921, 1–12.

Deflandre, G., Courteville, H., 1939. Note préliminaire sur les microfossiles des silex crétacés du Cambrésis (Preliminary note on the microfossils of the Cretaceous flint from Cambrésis). Bulletin de la société française de microscopie (Bulletin of the french society of microscopy) 8, 95–106, pl.2–4.

Deflandre, G., Cookson, I.C., 1955. Fossil microplankton from Australian late Mesozoic and Tertiary sediments. Australian Journal of Marine and Freshwater Research 6, 242–313, pl. 1–9.

Delcourt, A., Sprumont, G., 1955. Les spores et grains de pollen du Wealdien du Hainaut (The spores and pollen grains of Wealden of Hainaut). Memoires de la Société belge de Géologie (Memoirs of the Belgian Geolgoical Society) 5, 1–73, pl. 1–4.

Delcourt, A., Dettmann, M.E., Hughes, N.F., 1963. Revision of some Lower Cretaceous microspores from Belgium. Palaeontology 6, 282–292, pl. 42–45.

Dettmann, M.E., 1963. Upper Mesozoic microfloras from southeastern Australia. Proceedings of the Royal Society of Victoria 72, 1–148, pl. 1–27.

Dettmann, M.E., Clifford, H.T., 1992. Phylogeny and biogeography of *Ruffordia*, *Mohria* and *Anemia* (Schizaeaceae) and *Ceratopteris* (Pteridaceae): evidence from in situ and dispersed spores. Alcheringa: an Australian Journal of Palaeontology 16, 269–314.

Deunff, J., 1954. *Veryhachium*, genre nouveau d'hystrichosphères du Primaire (*Veryhachiu*m, a new kind of primary hystrichosphere). Compte rendu sommaire des séances de la Societe géologique de France (Summary report of the sessions of the Geological Society of France) 13, 305–306.

Dewing, K., Turner, E., Harrison, J. C., 2007. Geological history, mineral occurrences and mineral potential of the sedimentary rocks of the Canadian Arctic Archipelago. In: Goodfellow, W.D. (ed.), Mineral deposits of Canada: a synthesis of major deposit-types, district metallogeny, the evolution of geologic provinces, and exploration methods. Geological Association of Canada, Mineral Deposits Division, Special Publication 5, 733–753.

Dewing, K., Springer, A., Guest, B., Hadlari, T., 2016. Geological evolution and hydrocarbon potential of the salt-cored Hoodoo Dome, Svedrup Basin, Arctic Canada. Marine and Petroleum Geology 71, 134–148.

Dockman, D. M., Pearson, D. G., Heaman, L. M., Gibson, S. A., Sarkar, C., 2018. Timing and origin of magmatism in the Sverdrup Basin, northern Canada – implications for lithospheric evolution in the High Arctic Large Igneous Province (HALIP). Tectonophysics 742–743, 50–65.

Dodd, S.C., Mac Niocaill, C., Muxworthy, A.R., 2015. Long duration (>4 Ma) and steady-state volcanic activity in the Early Cretaceous Paraná–Etendeka Large Igneous Province: new palaeomagnetic data from Namibia. Earth and Planetary Science Letters 414, 16–29.

Dörhöfer, G., Davies, E.H., 1980. Evolution of archeopyle and tabulation in rhaetogonyaulacinean dinoflagellate cysts. Miscellaneous Publication, Royal Ontario Museum, Life Sciences Division, Toronto, Canada, 91 p.

Döring, H., 1964. Neue Sporengattungen und -arten aus dem Jura/Kreide-Grenzbereich Norddeutschlands (New spore genera and species from the Jura/Kreide border area in northern Germany). Monatsberichte der Deutschen Akademie der Wissenschaften zu Berlin (Monthly reports of the Germany Academy of Sciences on Berlin) 6, 37–45.

Dumitrescu, M., Brassel, S.C., Schouten, S., Hopmans, E.C., Sinninghe, D., Jaap, S., 2006. Instability in tropical Pacific sea-surface temperatures during the early Aptian. Geology 34, 833–836.

Duxbury, S., 1983. A study of dinoflagellate cysts and acritarchs from the Lower Greensand (Aptian to lower Albian) of the Isle of Wight, southern England. Palaeontographica Abteilung B, 186, 18–80, pl. 1–10.

Ebinghaus, A., Jolley, D.W., Hartley, A.J., 2015. Extrinsic forcing of plant ecosystems in a large igneous province: the Columbia River Flood Basalt Province, Washington State, USA. Geology 43, 1107–1110.

Eisenack, A., 1958. Mikroplankton aus dem norddeutschen Apt, nebst einigen Bemerkungen über fossile Dinoflagellaten (Microplankton from Apt in northern Germany, along with a few comments abaout fossil dinoflagellates). Neues Jahrbuch für Geologie und Paläontologie, Abhandlungen (New yearbook for geology and paleontology, treatises) 106, 383–422, pl. 21–27.

Eisenack, A., 1972. Kritische Bemerkung zur Gattung *Pterospermopsis* (Chlorophyta, Prasinophyceae). Critical remarks about *Pterospermopsis* (Chrolophyta, Prasinophyceae). Neues Jahrbuch für Geologie und Paläontologie, Monatshefte (New yearbook for geology and paleontology, monthly magazines), 1972-10, 596–601.

Eisenack, A., Cookson, I.C., 1960. Microplankton from Australian Lower Cretaceous sediments. Proceedings of the Royal Society of Victoria 72, 1–11, pl. 1–3.

Embry, A.F., 1985. Stratigraphic subdivision of the Isachsen and Christopher formations (Lower Cretaceous), Arctic Islands. Current Research, Part B, Geological Survey of Canada, Paper 85-1B, 239–246.

1271 Embry, A. F., 1991. Mesozoic history of the Arctic Islands. In Trettin, H. (ed.), Innuitian Orogen
1272 and Arctic Platform: Canada and Greenland; Geological Survey of Canada, Geology of Canada,
1273 no. 3, Ottawa, Canada, pp. 369–433.
1274
1275 Embry, A. F., Beauchamp, B., 2019. Chapter 14 Sverdrup Basin. In: Miall, A. (ed.), The
1276 sedimentary basins of the United States and Canada, 2nd Edition. Elsevier, Amsterdam, 559–592.
1277
1278 Embry, A.F., Dixon, J., 1990. The breakup unconformity of the Amerasia Basin, Arctic Ocean:
1279 evidence from Arctic Canada. Geological Society of America Bulletin 102, 1526–1534.
1280
1281 Embry, A.F., Osadetz, K.G., 1988. Stratigraphy and tectonic significance of Cretaceous volcanism
1282 in the Queen Elizabeth Islands, Canadian Arctic Archipelago. Canadian Journal of Earth Sciences
1283 25, 1209–1219.
1284
1285 Erba, E., 1994. Nannofossils and superplumes: The Early Aptian “nannoconid crisis”.
1286 Paleoceanography 9, 483–501.
1287
1288 Erba, E., Tremolada, F. 2004. Nannofossil carbonate fluxes during the Early Cretaceous:
1289 Phytoplankton response to nutrification episodes, atmospheric CO2, and anoxia,
1290 Paleoceanography 19, PA1008.
1291
1292 Erba, E., Bartolini, A., Larson, R.L., 2004. Valanginian Weissert Ocean Anoxic Event. Geology
1293 32, 149–152.

Erdtman, G., 1948. Did dicotyledonous plants exist in early Jurassic times? Geologiska Föreningens Förhandlingar (Geolgoical Association Negotiations) 70, 265–271.

Ernst, R., 2014. LIPs and environmental changes and catastrophes, in large igneous provinces. Cambridge University Press, Cambridge, 418–458.

Ernst, R.E., Youbi, N., 2017. How large igneous provinces affect global climate, sometimes cause mass extinctions, and represent natural markers in the geologic record. Palaeogeography, Palaeoclimatology, Palaeoecology 478, 30–52.

Estrada, S., Henjes-Kunst, F., 2004. Volcanism in the Canadian High Arctic related to the opening of the Arctic Ocean. Zeitschrift der Deutschen Geologischen Gesellschaft (Journal of the German Geological Society) 154, 579–603.

Estrada, S., Henjes-Kunst, F., 2013. 40Ar–39Ar and U–Pb dating of Cretaceous continental rift-related magmatism of the northeast Canadian Arctic margin. Zeitschrift der Deutschen Gesellschaft für Geowissenschaften (German Journal of Geosciences) 164, 107–130.

Evenchick, C.A., Embry, A.F., 2012a. Geology, Ellef Ringnes Island north, Nunavut. Geological Survey of Canada, Canadian Geoscience Map 86 (preliminary), scale 1:125,000. doi:10.4095/291565

1317 Evenchick, C.A., Embry, A.F., 2012b, Geology, Ellef Ringnes Island south, Nunavut. Geological
1318 Survey of Canada, Canadian Geoscience Map 87 (preliminary), scale 1:125,000.
1319 doi:10.4095/291566
1320
1321 Evenchick, C. A., Davis, W. J., Bédard, J. H., Hayward, N., Friedman, R. M., 2015. Evidence for
1322 protracted High Arctic Large Igneous Province magmatism in the central Sverdrup Basin from
1323 stratigraphy, geochronology, and paleodepths. Geological Society of America Bulletin 127, 1–25.
1324
1325 Evenchick, C.A., Galloway, J.M., Saumur, B.M., Davis, W.J., 2019. A revised stratigraphic
1326 framework for Cretaceous sedimentary and igneous rocks at Mokka Fiord, Axel Heiberg Island,
1327 Nunavut, with implications for the Cretaceous Normal Superchron. Canadian Journal of Earth
1328 Sciences 56, 158–174.
1329
1330 Fensome, R.A., Crux, J.A., Gard, I.G., MacRae, R.A., Williams, G.L., Thomas, F.C., Fiorini, F.,
1331 Wach, G., 2008. The last 100 million years on the Scotian Margin, offshore eastern Canada: an
1332 event-stratigraphic scheme emphasizing biostratigraphic data. Atlantic Geology 44, 93–126.
1333
1334 Fensome, R.A., Williams, G.L., MacRae, R.A., 2009. Late Cretaceous and Cenozoic fossil
1335 dinoflagellates and other palynomorphs from the Scotian Margin, offshore eastern Canada. Journal
1336 of Systematic Palaeontology 7, 1–79.
1337
1338 Fensome, R.A., Williams, G.L., Wood, S.E.L., Riding, J.B., 2019. A review of the areoligeracean
1339 dinoflagellate cyst *Cyclonephelium* and morphologically similar genera. Palynology 43, 1–71.

Filatoff, J., 1975. Jurassic palynology of the Perth Basin, Western Australia. Palaeontographica Abteilung B 154, 1–113, pl. 1–30.

Fischer, B.F.G., 1985. The geology of the area surrounding Bunde and Bukken fiords, northwestern Axel Heiberg Island, Canadian Arctic Archipelago. M.Sc. Thesis, University of Calgary, 114 p.

Föllmi, K.B., 2012. Early Cretaceous life, climate and anoxia. Cretaceous Research 35, 230–257.

Fowell, S.J., Olsen, P.E., 1993. Time calibration of Triassic/Jurassic microfloral turnover, eastern North America. Tectonophysics 222, 361–369.

Frakes, L.A., Francis, J.E., 1988. A guide to Phanerozoic cold polar climates from high latitude ice-rafting in the Cretaceous. Nature 333, 547–549.

Frebold, H., 1960. The Jurassic faunas of the Canadian Arctic: Lower Jurassic and lowermost Middle Jurassic ammonites. Geological Survey of Canada, Bulletin 59. 33 pp.

Frebold, H., 1975. The Jurassic faunas of the Canadian Arctic: Lower Jurassic ammonites, biostratigraphy and correlation. Geological Survey of Canada, Bulletin 243. 24 pp. (1 sheet).

Fricker, P.E. 1963. Geology of the Expedition area, western central Axel Heiberg Island, Canadian Arctic archipelago. Axel Heiberg Island Research Reports, McGill University, Montreal, Geology 1, 156 pp.

Gale, A.S., Mutterlose, J., Batenburg, S. with Gradstein, F.M., Agterberg, F.P., Ogg, J.G., Petrizzo, M.R. (contributors). 2020. Chapter 27: The Cretaceous Period. In: Gradstein, F.M., Ogg, J.G., Schmitz, M.D., Ogg, G. (eds.), The Geological Time Scale, Book Volume 2, Part III. Geological Periods Phanerozoic, pp. 1023-1086.

Galloway, J.M., Sweet, A.R., Pugh, A., Schöder-Adams, C.J., Swindles, G.T., Haggart, J.W., Embry, A.F., 2012. Correlating middle Cretaceous palynological records from the Canadian High Arctic based on a section from the Sverdrup Basin and samples from the Eclipse Trough. Palynology 36, 277–302.

Galloway, J.M., Sweet, A., Sanei, H., Dewing, K., Hadlari, T., Embry, A.F., Swindles, G.T., 2013. Middle Jurassic to Lower Cretaceous paleoclimate of Sverdrup Basin, Canadian Arctic Archipelago inferred from the palynostratigraphy. Marine and Petroleum Geology 44, 240–255.

Galloway, J.M., Tullius, D.N., Evenchick, C.A., Swindles, G.T., Hadlari, T., Embry, A., 2015. Early Cretaceous vegetation and climate change at high latitude: palynological evidence from Isachsen Formation, Arctic Canada. Cretaceous Research 56, 399–420.

Galloway, J.M., Vickers, M., Price, G.D., Poulton, T.P., Grasby, S.E., Hadlari, T., Beauchamp, B., Sulphur, K., 2019. Finding the VOICE: organic carbon isotope chemostratigraphy of the Late Jurassic–Early Cretaceous of arctic Canada. Geological Magazine 1–15, doi.10.1017/S0016756819001316.

Gauch, H.G. Jr., 1982. Noise reduction by Eigenvector ordinations. Ecology 63, 1643–1649.

Gocht, H., 1957. Mikroplankton aus dem nordwestdeutschen Neokom (Teil I) (Microplankton from the Northwest German Neocomian (Part I). Paläontologische Zeitschrift (Paleontological Journal) 31, 163–185, pl. 18–20.

Gocht, H., 1959. Mikroplankton aus dem nordwestdeutschen Neokom (Teil II) (Microplankton from the Northwest German Neocomian (Part II). Paläontologische Zeitschrift (Paleontological Journal) 33, 50–89, pl. 3–8.

Grasby, S.E., Sanei, H., Beauchamp, B., 2011. Catastrophic dispersion of coal fly ash into oceans during the latest Permian extinction. Nature Geoscience 4, 104–107.

Grasby, S.E., McCune, G.E., Beauchamp, B., Galloway, J.M., 2017. Lower Cretaceous cold snaps led to widespread glendonite occurrences in the Sverdrup Basin, Canadian High Arctic. Geological Society of America Bulletin 129, 771–787.

Grimm, E.C., 1987. CONISS: a FORTRAN 77 program for stratigraphically constrained cluster analysis by the method of incremental sum of squares. Computers and Geoscience 13, 13–35.

Grimm, E., 1993–2001. TILIA: a pollen program for analysis and display. Illinois State Museum, Springfield.

Gröcke, D.R., Price, G.D., Robinson, S.A., Baraboshkin, E.Y., Mutterlose, J., Ruffell, A., 2005. The upper Valanginian (Early Cretaceous) positive carbon-isotope event recorded in terrestrial plants. Earth and Planetary Science Letters 240, 495–509.

Hadlari, T., Midwinter, D., Galloway, J. M., Durbano, A. M., 2016. Mesozoic rift to post-rift tectonostratigraphy of the Sverdrup Basin, Canadian Arctic. Marine and Petroleum Geology 76, 148–158.

Hadlari, T., Dewing, K., Matthews, W.A., Alonso-Torres, D., Midwinter, D., 2018. Early Triassic development of a foreland basin in the Canadian High Arctic: implications for a Pangean Rim of Fire. Tectonophysics 736, 75–84.

Harding, I.C., 1990b. A dinocyst calibration of the European Boreal Barremian. Palaeontographica, Abteilung B 218, 1–76, pl.1–31.

Harland, M., Francis, J.E., Brentnall, S.J., Beerling, D.J., 2007. Cretaceous (Albian–Aptian) conifer wood from Northern Hemisphere high latitudes: korest composition and palaeoclimate. Review of Palaeobotany and Palynology 143, 167–196.

Harrison, J.C., Mayr, D.H., McNeil, D.H., Sweet, A.R., McIntyre, D.J., Eberle, J.J., Harington, C.R., Chalmers, J.A., Dam, G., Nøhr-Hansen, H., 1999. Correlation of Cenozoic sequences of the Canadian Arctic region and Greenland; implications for the tectonic history of northern North America. Bulletin of Canadian Petroleum Geology 47, 223–254.

Hedlund, R.W., 1965. *Sigmopollis hispidus* gen. et sp. nov. from Miocene sediments, Elko County, Nevada. Pollen et Spores 7, 89–92.

Heimdal, T.H., Svensen, H.H., Ramezani, J., Iyer, K., Pereira, E., Rodrigues, R., Jones, M.T., Callegaro, S., 2018. Large-scale sill emplacement in Brazil as a trigger for the end-Triassic crises. Nature: Scientific Reports 8, 141.

Helby, R., 1987. *Muderongia* and related dinoflagellates of the latest Jurassic to Early Cretaceous of Australasia. In: Jell, P.A. (ed.), Studies in Australian Mesozoic palynology. Memoir of the Association of Australasian Palaeontologists 4, 297–336.

Helenes, J., 1984. Morphological analysis of Mesozoic-Cenozoic *Cribroperidinium* (Dinophyceae), and taxonomic implications. Palynology 8, 107–137, pl.1–5.

Herngreen, G.F.W., Kedves, M., Rovnina L.V., Smirnova S.B., 1996. Cretaceous palynofloral provinces. In: Jansonius J., McGregor D.C. (eds.), Palynology: principles and applications, volume 3. American Association of Stratigraphic Palynologists Foundation, Salt Lake City, 1157–1188.

Herrle, J. O., Kosler, P., Bollmann, J., 2010. Palaeoceanographic differences of early late Aptian black shale events in the Vocontian Basin (SE France). Palaeogeography, Palaeoclimatology, Palaeocology 297, 367–376.

Herrle, J., Schröder-Adams, C.J., Davis, W., Pugh, A.T., Galloway, J.M., Fath, J., 2015. Mid-Cretaceous High Arctic stratigraphy, climate and oceanic anoxic events. Geology 43, 403–406.

Hesselbo, S.P., Ogg, J.G., Ruhl, M. with Hinnov, L.A., Huang, C.J. (contributors). 2020. Chapter 25: The Jurassic Period. In: Gradstein, F.M., Ogg, J.G., Schmitz, M.D., Ogg, G. (eds.), The Geological Time Scale, Book Volume 2, Part III. Geological Periods Phanerozoic pp. 955–1021.

Heywood, W.W., 1957. Isachsen Area, Ellef Ringes Island, District of Franklin, Northwest Territories: Geological Survey of Canada Special Paper 56-8, 36 p.

Hochuli, P.A., Megegatti, A.P., Weissert, H., Riva, A., Erba, E., Premoli Silva, I., 1999. Episodes of high productivity and cooling in the early Aptian Alpine Tethys. Geology 27, 657–660.

Hochuli, P.A., Vigran, J.O., Hermann, E., Bucher, H., 2010. Multiple climatic changes around the Permian–Triassic boundary event revealed by an expanded palynological record from mid-Norway. Geological Society of America Bulletin 122, 884–96.

Holland, M.M., Bitz, C.M., 2003. Polar amplification of climate change in coupled models. Climate Dynamics 21, 221–232.

Holland, S. M., Miller, A.I., Meyer, D.L., Dattilo, B.F., 2001.The detection and importance of subtle biofacies within a single lithofacies: the Upper Ordovician Kope Formation of the Cincinnati, Ohio region. Palaios 16, 205–217.

Hopkins, W.S. Jr., 1971. Palynology of the Lower Cretaceous Isachsen Formation on Melville Island, District of Franklin. In: Norford, B.S., Pedder, A.E.H., Ormiston, A.R., Eyer, J.A., Nassichuk, W.W., Spinosa, C., Ross, C.A., Hopkins, W.S., Jr. (eds.), Contributions to Canadian Paleontology. Geological Survey of Canada, Bulletin 197, 109–127.

Hopkins, W.S. Jr., 1973. Some spores and pollen from the Christopher Formation (Albian) of Ellef and Amund Ringnes Island, and northwestern Melville Island. Geological Survey of Canada, Paper 73-12, 39 pp.

Hu, X., Zhao, K., Yilmaz, I.O., Li, Y. 2017. Stratigraphic transition and palaeoenvironmental changes from the Aptian Oceanic Anoxic Event 1a (OAE1a) to the oceanic red bed 1 (ORB1) in the Yenicesihlar section, central Turkey. Cretaceous Research 38, 40–51.

Ibrahim, A.C., 1933. Sporenformen des Äegirhorizonts des Ruhr Reviers. Triltsch, Wurzburg, Germany, 46 pp.

Islam, M.A., 1993. Review of the fossil dinoflagellate *Cleistosphaeridium*. Revista española de micropaleontología (Spanish journal of micropaleontology) 25, 81–94, pl.1.

Jahren, A.H., Arens, N.C., Sarmiento, G., Guerrero, J., Amundson, R., 2001. Terrestrial record of methane hydrate dissociation in the Early Cretaceous. Geology 29, 159–162.

Jain, K.P., 1977. Additional dinoflagellates and acritarchs from Grey Shale Member of Dalmiapuram Formation, south India. The Palaeobotanist, 24, 170–194, pl.1–6.

Jain, K.P.,Millepied, P., 1973. Cretaceous microplankton from Senegal Basin, NW Africa. 1. Some new genera, species and combinations of dinoflagellates. The Palaeobotanist 20, 22–32, pl.1–3.

Janasi, V., de Freitas, V.A., Heaman, L.H., 2001. The onset of flood basalt volcanism, northern Paranó Basin, Brazil: a precise U–Pb baddeleyite/zircon age for a Chapecó-type dacite. Earth and Planetary Science Letters 302, 147–153.

Jansonius, J., 1986. Re-examination of Mesozoic Canadian dinoflagellate cysts published by S.A.J. Pocock (1962, 1972). Palynology 10, 201–223, pl.1–6.

Jarvis, I., Lignum, J.S., Gröcke, D.R., Jenkyns, H.C., 2011. Black shale deposition, atmospheric CO_2 drawdown, and cooling during the Cenomanian–Turonian oceanic anoxic event. Palaeoceanography 26, PA3201.

Jeletzky, J.A., 1973. Biochronology of the marine boreal latest Jurassic, Berriasian and Valanginian in Canada. In Casey, R., Rawson, P.F. (eds), The Boreal Lower Cretaceous, Seel House Press, Liverpool, p. 41–80.

Jenkyns, H.C., 1995. Carbon-isotope stratigraphy and paleoceanographic significance of the Lower Cretaceous shallow-water carbonates of Resolution Guyot, Mid-Pacific Mountains. In: Winterer, E.L., Sager, W.W., Firth, J.V., Sinton, J.M. (Eds.), Proceedings of the Ocean Drilling Program Scientific Results 143. 99–104.

Jenkyns, H.C., 2010. Geochemistry of oceanic anoxic events. Geochemistry, Geophysics, Geosystems 11, Q03004.

Jenkyns, H., 2018. Transient cooling episodes during Cretaceous oceanic events with special reference to OAE 1a (Aptian). Philosophical Transactions of the Royal Society, A: Mathematical, Physical and Engineering Sciences 376, 20170073.

Jenkyns, H. C., Wilson, P. A., 1999. Stratigraphy, paleoceanography, and evolution of Cretaceous Pacific guyots: relics from a greenhouse Earth. American Journal of Science 299, 341–392.

1540 Jenkyns, H.C., Dickson, A.J., Ruhl, M., Van Den Boorn, S.H.J.M., 2017. Basalt- seawater
1541 interaction, the Plenus Cold Event, enhanced weathering and geochemical change: deconstructing
1542 Oceanic Anoxic Event 2 (Cenomanian–Turonian, Late Cretaceous). Sedimentology 64, 16–43.
1543
1544 Jolley, D.W., 1997, Palaeosurface palynofloras of the Skye Lava Field and the age of the British
1545 Tertiary volcanic province. In Widdowson, M., (ed.), Palaeosurfaces: recognition, reconstruction
1546 and palaeoenvironmental interpretation. Geological Society of London Special Paper 120, 67–94.
1547 doi:10.1144/GSL.SP.1997.120.01.06.
1548
1549 Jolley, D.W., Widdowson, M., Self, S., 2008. Volcanogenic nutrient fluxes and plant ecosystems
1550 in large igneous provinces: an example from the Columbia River Basalt Group. Journal of the
1551 Geological Society, London 165, 955–966.
1552
1553 Jones, M.T., Jerram, D.A., Svensen, H.H., Grove, C., 2016. The effects of large igneous provinces
1554 on the global carbon and sulphur cycles. Palaeogeography, Palaeoclimatology, Palaeoecology 441,
1555 4–21.
1556
1557 Jowitt, S.W., Williamson, M.-C., Ernst, R.E., 2014. Geochemistry of the 130 to 80 Ma Canadian
1558 High Arctic Large Igneous Province (HALIP) event and implications for Ni–Cu–PGE
1559 prospectivity. Economic Geology and the Bulletin for the Society of Economic Geologists 109,
1560 281–750.
1561
1562 Keller, C.E., Hochuli, P.A., Weissert, H., Bernasconi, S.M., Giorgioni, M., Garcia, T.I. 2011.

A volcanically induced climate warming and floral change preceded the onset of OAE1a (Early Cretaceous. Palaeogeography, Palaeoclimatology, Palaeoecology 305, 43–49.

Kemper, E., 1975, Upper Deer Bay Formation (Berriasian-Valanginian) of Sverdrup Basin and Biostratigraphy of the Arctic Valanginian: Geological Survey of Canada Paper 75-1B, p. 245–254.

Kessels, K., Mutterlose, J.,m Michalzik, D., 2006. Early Cretaceous (Valanginian-Hauterivian) calcareous nannofossils and isotopes of the northern hemisphere: proxies for the udnerstanding of Cretaceous climate. Lethaia 39, 157–172.

Kingsbury, C., Kamo, S. L., Ernst, R. E., Söderlund, U., Cousens, B. L., 2018. U–Pb geochronology of the plumbing system associated with the Late Cretaceous Strand Fiord Formation, Axel Heiberg Island, Canada: part of the 130–90 Ma High Arctic Large Igneous Province. Journal of Geodynamics 118, 106–117.

Krutzsch, W., 1963. Atlas der Mittel- und Jungtertiären Dispersen Sporen und Pollen sowie der Mikroplanktonformen des Nördlichen Mitteleuropas, II, Die Sporen der Anthocerotaceae und der Lycopodiaceae. VEB Deutscher Verlag der Wissenschaften, Berlin, 141 p.

Krutzsch, W., Pacltová, B., 1990. Die Phytoplankton-Mikroflora aus den Pliozänen Süsswasserablagerungen des Cheb-Beckens (Westböhmen, ÈSFR) (The phytoplankton microflora

1585 from the Pliocene freshwater deposits of the Cheb Basin (West Bohemia). Acta Universitatis
1586 Carolinae — Geologica 4, 345–420.
1587
1588 Kuhnt, W., Holbourn, A., Moullade, M., 2011. Transient global cooling at the onset of early Aptian
1589 Oceanic Anoxic Event (OAE) 1a. Geology, 39, 323–326.
1590
1591 Larson, R.L., 1991. Latest pulse of Earth: Evidence for a mid Cretaceous superplume. Geology
1592 19, 547–550.
1593
1594 Lentin, J.K., Vozzhennikova, T.F., 1990. Fossil dinoflagellates from the Jurassic, Cretaceous and
1595 Paleogene deposits of the USSR — a re-study. American Association of Stratigraphic
1596 Palynologists, Contributions Series, no.23, 221 p., pl.1–16.
1597
1598 Lentin, J.K., Williams, G.L., 1976. A monograph of fossil peridinioid dinoflagellate cysts. Bedford
1599 Institute of Oceanography, Report Series, no.BI-R-75-16, 237 p. [Cover date 1975, issue date
1600 1976]
1601
1602 Lentin, J.K., Williams, G.L., 1981. Fossil dinoflagellates: index to genera and species, 1981
1603 edition. Bedford Institute of Oceanography, Report Series BI-R-81-12, 345 p.
1604 Lenz, O.K., Wilde, V., Riegel, W., 2007. Recolonization of a Middle Eocene volcanic site:
1605 quantitative palynology of the initial phase of the maar lake of Messel (Germany). Review of
1606 Palaeobotany and Palynology 145, 217–242.
1607

Lindström, S., Pedersen, G.K., van de Schootbrugge, B., Hansen, K.H., Kuhlmann, N., Thein, J., Johansson, L., Petersen, H.I., Alwmark, C., Dybkjær, K., Weibel, R., Erlström, M., Nielsen, L.H., Oschmann,W., Tegner, C., 2015. Intense and widespread seismicity during the end-Triassic mass extinction due to emplacement of a large igneous province. Geology 43, 387–390.

Lindström, S., Sanei, H. van de Schootbrugge, B., Pedersen, G.K., Lesher, C.E., Tegner, C., Heunisch, C., Dybkjær, K., Outridge, P.M., 2019. Volcanic mercury and mutagenesis in land plants during the end-Triassic mass extinction. Scientific Advances 5, eaaw4018.

Lini, A., Weissert, H., Erba, E., 1992. The Valanginian carbon isotope event: a first episode of greenhouse climate conditions during the Cretaceous. Terra Nova 4, 374–384.

Lorenzen, J., Kuhnt, W., Holbourn, A., Flögel, S., Moullade, M., Tronchetti, G. 2013. A new sediment core from the Bedoulian (lower Aptian) stratotype at Roquefort–La Bédoule, SE France. Cretaceous Research 39, 6–16.

Maher, H.D., Jr. 2001. Manifestations of the Cretaceous High Arctic Large Igneous Province in Svalbard. Journal of Geology 109, 91–104.

Mahmoud, M.S., 1998. Palynology of middle Cretaceous–Tertiary sequence of Mersa Matruh-1 well, northern Western Desert, Egypt. Neues Jahrbuch für Geologie und Paläontologie Abhandlungen (New yearbook for geology and paleontology treatistes) 209, 79–104.

1631 Mallik, A.U., 1995. Conversion of temperate forests into heaths: Role of ecosystem disturbance
1632 and ericaceous plants. Environmental Management 19, 675–684.
1633
1634 Malkoč, M., Mutterlose, J., Pauly, S. 2010. Timing of the early Aptian $\delta^{13}C$ excursion in the Boreal
1635 Realm. Newsletters on Stratigraphy 43, 251–273.
1636
1637 Mantell, G.A., 1850. A pictorial atlas of Fossil Remains Consisting of Coloured Illustrations
1638 Selected from Parkinson's "Organic Remains of a Former World", and Artis's "Antediluvian
1639 Phytology". xii+207 p., 74 pl.; Henry G. Bohn, London, UK.
1640
1641 Martinez, M., Deconinck, J-F., Pellenard, P., Riquier, L., Company, M., Reboulet, S., Moiroud,
1642 M., 2015. Astrochronology of the Valanginian-Hauterivian stages (Early Cretaceous):
1643 Chronological relationships between the Paraná-Etendeka large igneous province and the Weissert
1644 and the Faraoni events. Global and Planetary Change 131, 158–173.
1645
1646 McArthur, J.M., Mutterlose, J., Price, G.D., Rawson, P.F., Ruffell, A., Thirlwall, M.F., 2004.
1647 Belemnites of Valanginian, Hatuerivian and Barremian age: Sr-isotope stratigraphy, composition
1648 ($^{87}Sr/^{86}Sr$, $\delta^{13}C$, $\delta^{18}O$, Na, Sr, Mg), and palaeo-oceanography. Palaeogeography,
1649 Palaeoclimatology, Palaeoecology 202, 253–272.
1650
1651 McCabe, P.J., Parrish, J.T., 1992. Controls on the distribution and quality of Cretaceous coals.
1652 Geological Society of America Special Papers 267, 407 pp.
1653

McAnena, A., Flögel, S., Hofmann, Herrle, J.O., Griesand, A., Pross, J., Talbot, H.M., Rethemeyer, J., Wallmann, K., Wagner, T., 2013. Atlantic cooling associated with a marine biotic crisis during the mid-Cretaceous period. Nature Geoscience 6, 558–561.

McElwain, J.C., Beerling, D.J., Woodward, F.I., 1999. Fossils plants and global warming at the Triassic–Jurassic boundary. Science 285, 1386–1390.

McGregor, D.C., 1965. Triassic, Jurassic and Lower Cretaceous spores and pollen of arctic Canada. Geological Survey of Canada, Paper 64–55, 32 p.

McIntyre, D.J., 1984. Palynological report on seven Isachsen Formation samples from Glacier Fiord, Axel Heiberg Island, N.W.T. (NTS 59E/10). Geological Survey of Canada (Calgary), Paleontology Report 6-DJM-1984, 3 p.

McMillan, N.J., 1963. Slidre River. In: Fortier, Y.O., Blackadar, R.G., Glenister, B.F., Greiner, H.R., McLaren, D.J., McMillan, N.J., Norris, A., Roots, E.F., Souther, J.G., Thorsteinsson, R., Tozer, E.T.. (eds.), Geology of the north-central part of the Arctic Archipelago, N.W.T. (Operation Franklin). Geological Survey of Canada, Memoir 320, 704 pp. (25 sheets).

Menegatti, A.P., Weissert, H., Brown, R.S., Tyson, R.V., Farrimond, P., Strasser, A., Caron, M. 1998. High-resolution δ13 C stratigraphy through the early Aptian "Livello Selli" of the Alpine Tethys. Paleoceanography 13, 530–545.

Meneley, R.A., Henao, D., Merritt, R.K., 1975. The northwest margin of the Sverdrup Basin in Canada – continental margins and offshore petroleum exploration. Canadian Society of Petroleum Geologists 4, 531–544.

Meyen, F.J.F., 1829. Beobachtungen über einige niedere Algenformen. Nova Acta Physico-Medica Academiae Caesareae Leopoldino-Carolinae Naturae 14, 768–778, pl. 43.

Midtkandal et al., I., Svensen, H.H., Planke, S., Corfu, F., Polteau, S., Torsvik, T.H., Faleide, J.I., Grundvåg, S., Selnes, H., Kürschner, W., Olaussen, S. 2016. The Aptian (Early Cretaceous) Oceanic Anoxic Event (OAE1a) in Svalbard, Barents Sea, and the absolute age of the Barremian–Aptian boundary. Palaeogeography, Palaeoclimatology, Palaeoecology 463, 126–135.

Midwinter, D., Hadlari, T., Davis, W. J., Dewing, K., Arnott, R. W. C., 2016. Dual provenance signatures of the Triassic northern Laurentian margin from detrital zircon U–Pb and Hf isotope analysis of Triassic–Jurassic strata in the Sverdrup Basin. Lithosphere 8, 668–683.

Möller, C., Mutterlose, J., Alsen, P., 2015. Intergrated stratigraphy of Lower Cretaceous sediments (Ryazanian–Hauterivian) from North-East Greenland. Palaeogeography, Palaeoclimatology, Palaeoecology 437, 85–97.

Moore, P.R., 1981. Mesozoic stratigraphy in the Blue Mountains and Krieger Mountains, northern Ellesmere Island, Arctic Canada: a preliminary account. Geological Survey of Canada Paper 81–1A, 95-101.

Mutterlose, J., Bottini, C., 2013. Early Cretaceous chalks from the North Sea giving evidence for global change. Nature Communications 4, 1686.

Mutterlose, J., Bottini, C., Schouten, S., Sinninghe Damsté, J.S., 2014. High sea-surface temperatures during the early Aptian Oceanic Anoxic Event 1a in the Boreal Realm. Geology 42, 439–442.

Naafs, B., Pancost, R., 2016. Sea-surface temperature evolution across Aptian Oceanic Anoxic Event 1a. Geology 44, 959–962.

Naumova, S.N., 1939. Spores and pollen of the coals of the U.S.S.R. Report of the XVII International Geological Congress, Moscow, 1937, 1, 353–364.

Naumova, S.N., 1953. Sporovo pyltsevye kompleksy verkhnego devona Russkoi platformy i ikh znachenie dlya stratigrafii (Spore-pollen complexes of the Upper Devonian of the Russian Platform and their significant for stratigraphy). Akademiya Nauk SSSR, Institut Geologischeskikh Nauk, Trudy, Seriya Geologicheskaya (USSR Academy of Sciences, Institute of Geological Sciences, Proceedings, Geological Series), no. 60, 1 154.

1721 Neale, J.W. and Sarjeant, W.A.S., 1962. Microplankton from the Speeton Clay of Yorkshire.
1722 Geological Magazine, 99, p.439–458, pl.19–20.
1723
1724 Newton, E.T., 1875. On "tasmanite" and Australian "white coal". Geological Magazine 2, 337–
1725 342, pl.10.
1726
1727 Nichols, D.J., Jarzen, D.M., Orth, C.J., Oliver, P.O., 1986. Palynological and iridium anomalies at
1728 Cretaceous–Tertiary boundary, south-central Saskatchewan. Science, 231, 714–717.
1729
1730 Nilsson, T., 1958. Über das Vorkommen eines mesozoischen Sapropelgesteins in Schonen (About
1731 the occurrence of a Mesozoic sparopel rock in Scania). Lunds Universitets Arsskrift, Ny Följd
1732 (Lund University Journal, New Order), Avd. 2, 54, 1–112, pl.1–8.
1733
1734 Nøhr-Hansen, H., 1993. Dinoflagellate cyst stratigraphy of the Barremian to Albian, Lower
1735 Cretaceous, North-East Greenland. Grønlands Geologiske Undersøgelse (Greenland Geological
1736 Survey), Bulletin 166, 1–171, pl.1–30.
1737
1738 Nøhr-Hansen, H., McIntyre, D.J., 1998. Upper Barremian to Upper Albian (Lower Cretaceous)
1739 dinoflagellate cyst assemblages, Canadian Arctic Archipelago. Palynology 22, 143–166.
1740
1741 Nøhr-Hansen, H., Williams, G.L., Fensome, R.A. 2016. Biostratigraphic correlation of the western
1742 and eastern margins of the Labrador–Baffin Seaway and implications for the regional geology.
1743 Geological Survey of Greenland and Denmark Bulletin 37, 74 p.

Oksanen, J., Blanchet, F.G., Friendly, M., Kindt, R., Legendre, P., McGlinn, D., Minchin, P.R., O'Hara, R.B., Simpson, G.L., Solymos, P., Stevens, H.H., Szoecs, E., Wagner, H. 2017. Vegan: Community Ecology Package, R package version 2.4-4. https://CRAN.R-project.org/package=vegan.

Olierook, H.K.H., Jourdan, Merle, R.E. 2019. Age of the Barremian-Aptain boundary and onset of the Cretaceous Normal Superchron. Earth-Science Reviews 197, 102906.

Omma, J. E., Pease, V., Scott, R. A., 2011. U–Pb SIMS zircon geochronology of Triassic and Jurassic sandstones on northwestern Axel Heiberg Island, northern Sverdrup Basin, Arctic Canada. In: Spencer, A.M., Embry, A.F., Gautier, A.V., Stoupakova, A.V., Sørensen, K (eds.), Arctic petroleum geology. Geological Society of London, Memoir 35, 559–566.

Page, C.N., 2002. Ecological strategies in fern evolution: a neopteridological overview. Review of Palaeobotany and Palynology 119, 1–33.

Pauly, S., Mutterlose, J., Wray, D.S., 2013. Palaeoceanography of Lower Cretaceous (Barremian–lower Aptian) black shales from northwest Germany evidenced by calcareous nannofossils and geochemistry. Cretaceous Research 42, 28–43.

Pflug, H.D., 1953. Zur Entstehung und Entwicklung des angiospermiden Pollens in der Erdgeschichte (On the origin and development of angiospermid pollen in Earth's history). Palaeontographica Abteilung B 95, 60–171, pl.15–25.

Planke, S., Polteau, S., Senger, K., Svensen, H.H., Faleide, J.I., Myklebust, R., Tegner, C. 2017. HALIP intrusive and extrusive complexes of Svalbard and the Barents Sea. In: Williamson, M.C. (ed.), GEM 2 High Arctic Large Igneous Province (HALIP) activity: workshop report. Geological Survey of Canada, Open File 8151, 60 p.

Playford, G., 1971. Palynology of Lower Cretaceous (Swan River) strata of Saskatchewan and Manitoba. Palaeontology 14, 533–565, pl.103–107.

Pocock, S.A.J., 1962. Microfloral analysis and age determination of strata at the Jurassic–Cretaceous boundary in the western Canada plains. Palaeontographica Abteilung B 111, 1–95, pl.1–15.

Pocock, S.A.J., 1964. Pollen and spores of the Chlamydospermidae and Schiziaceae from Upper Mannville strata of the Saskatoon area of Saskatchewan. Grana Palynologica 5, 129-209.

Podlaha, O.G., Mutterlose, J., Veizer, J., 1998. Preservation of $\delta^{18}O$ and $\delta^{13}C$ in belemnite rostra from the Jurassic/Early Cretaceous successions. American Journal of Science 298, 324–347.

Polteau, S., Hendriks, B.W.H., Planke, S., Ganerød, M., Corfu, F., Faleide, J.I., Midtkandal, I., Svensen, H.S., Myklebust, R., 2016. The Early Cretaceous Barents Sea Sill Complex: distribution, $^{40}Ar/^{39}Ar$ geochronology, and implications for carbon gas formation. Palaeogeography, Palaeoclimatology, Palaeoecology 441, 83–95.

Potonié, R., 1931. Zur Mikroskopie der Braunkohlen: tertiäre Sporen und Blütenstaubformen (For microscopy of brown coal: tertiary spores and pollen forms). Zeitschrift für Braunkohle (Magazine for lignite) 27, 554–556.

Potonié, R., 1956. Synopsis der Gattungen der Sporae dispersae. I. Teil: Sporites (Synopsis of the genera of the sporae dispersae, Part 1: Sporites). Geologisches Jahrbuch, Beihefte (Geological Yearbook, Booklet) 23, 1–103, pl. 1–11.

Potonié, R., 1958. Synopsis der Gattungen der Sporae dispersae. II. Teil: Sporites (Nachträge), Saccites, Aletes, Praecolpates, Polyplicates, Monocolpates (Synopsis of the genera of the sporae dispersae, Part II: Sporites (supplements), Saccites, Aletes, Praecolpates, Polyplicates, Monocolpates). Geologisches Jahrbuch, Beihefte (Geological Yearbook, Booklet) 31, 1–113, pl. 1–11.

Potonié, R., Gelletich, J., 1933. Über Pteridophyten-Sporen einer Eozänen Braunkohle aus Dorog in Ungarn (About pteridophyte spores of an Eocene lignite from Dorog in Hungary). Sitzungsberichte Gesellschaft, Naturforsch Freunde zu Berlin (Meeting reports society, natural science friends to Berlin), 1932, 517–528, 2 pl.

Potonié, R., Kremp, G., 1954. Die Gattungen der paläozoischen Sporae dispersae und ihre Stratigraphie (The genera of the Paleozoic Sporae dispersae and their stratigraphy). Geologisches Jahrbuch (Geological Yearbook) 69, 111–194, pl. 4–20.

Potonié, R., Thomson, P., Thiergart, F., 1950. Zur Nomenklatur und Klassifikation der neogenen Sporomorphae (Pollen und Sporen) (On the nomenclature and classification of neogenic sporomorphae (pollen and spores)). Geologisches Jahrbuch (Geological Yearbook) 65, 35–70, pl. 3.

Poulson, C.J., Zhou, J., 2013. Sensitivity of Arctic climate variability to mean state: insights from the Cretaceous. Journal of Climate 26, 7003–7022.

Price, G. D., 1999. The evidence and implications of polar ice during the Mesozoic. Earth-Science Reviews, 48, 183–210.

Price, G.D., 2003. New constraints upon isotope variation during the Early Cretaceous (Barremian-Cenomanian) from the Pacific Ocean. Geological Magazine 140, 513–522.

Price, G.D., Nunn, E.V., 2010. Valanginian isotope variation in glendonites and belemnites from arctic Svalbard: transient glacial temperatures during the Cretaceous greenhouse. Geology 38, 251–254.

Price, G.D, Janssen, N.M.M., Martinez, M., Company, M., Vandevelde, J.H., Grimes, S.T., 2018. A high-resolution belemnite geochemical analysis of Early Cretaceous (Valanginian-Hauterivian) environmental and climatic pertubations. Geochemistry, Geophysics, Geosystems 19, 3832–3843.

Pucéat, E., Lécuyer, C., Sheppard, S.M.F., Dromart, G., Reboulet, S., Grandjean, P., 2003. Thermal evolution of Cretaceous Tethyan marine waters inferred from oxygen isotope composition of fish tooth enamels. Paleoceanography 18, 1029.

Pugh, A.T., Schröder-Adams, C.J., Carter, E.S., Herrle, J.O., Galloway, J., Haggart, J.W., Andrews, J.L., Hatsukano, K., 2014. Cenomanian to Santonian radiolarian biostratigraphy, carbon isotope stratigraphy and paleoenvironments of the Sverdrup Basin, Ellef Ringnes Island, Nunavut, Canada. Palaeogeography, Palaeoclimatology, Palaeoecology 413, 101–122.

R Core Team, 2017. R: A language and environment for statistical computing. R Foundation for Statistical Computing, Vienna, Austria. URL https://www.R-project.org/

Ravn, R.L., 1995. Miospores from the Muddy Sandstone (upper Albian), Wind River Basin, Wyoming, USA. Palaeontographica Abteilung B 234, 41–91.

Reissinger, A., 1950. Die "Pollenanalyse" ausgedehnt auf alle Sedimentgesteine der geologischen Vergangenheit (The “pollen analysis” extended to all sedimentary rocks in the geological past). Palaeontographica Abteilung B 90, 99–126, pl. 11–19.

Ricketts, B., Osadetz, K.G., Embry, A.F., 1985. Volcanic style in the Strand Fiord Formation (Upper Cretaceous), Axel Heiberg Island, Canadian Arctic Archipelago. Polar Research 3, 107–122.

Rocha, B.C., Davies, J.H.F., Janasi, V.Q., Schaltegger, U., Nardy, A.J.R., Greber, N.D., Lucchetti, A.C.F., Polo, L.A., 2020. Rapid eruption of silica magmas from the Paraná magmatic province (Brazil) did not trigger the Valanginian event. Geology 48, 1174–1178.

Rogov, M.A., Ershova, V.B., Shchepetova, V.A., Zakharov, B.G., Pokrovsky, B.G., Khudoley, A.K. 2017. Earliest Cretaceous (late Berriasian) glendonites from Northeast Siberia revise the timing of initiation of transient Early Cretaceous cooling in the high latitudes. Cretaceous Research 71, 102–112.

Ross, N.E., 1949. On a Cretaceous pollen and spore bearing clay deposit of Scania. Bulletin of the Geologicial Institute of the University of Uppsala, 34, 25–43, pl. 1–3.

Rouse, G.E., 1959. Plant microfossils from Kootenay coal measures strata of British Columbia. Micropaleontology 5, 303–324.

Rückheim, S., Bornemann, A., Mutterlose, J., 2006. Planktic foraminifera from the mid-Cretaceous (Barremian–early Albian) of the North Sea Basin: palaeoecological and palaeoceanographic implications. Marine Micropaleontology 58, 83–102.

Sanei, H., Grasby, S.E., Beauchamp, B., 2012. Latest Permian mercury anomalies. Geology 40, 63–66.

Sarjeant, W.A.S., 1966a. Dinoflagellate cysts with *Gonyaulax*-type tabulation. In: Davey, R.J., Downie, C., Sarjeant, W.A.S., Williams, G.L. (eds.), Studies on Mesozoic and Cainozoic dinoflagellate cysts; British Museum (Natural History) Geology, Bulletin, Supplement 3, 107–156.

Sarjeant, W.A.S., 1966b. Further dinoflagellate cysts from the Speeton Clay. In: Davey, R.J., Downie, C., Sarjeant, W.A.S., Williams, G.L. (eds.), Studies on Mesozoic and Cainozoic dinoflagellate cysts; British Museum (Natural History) Geology, Bulletin, Supplement 3, 199–214.

Sarjeant, W.A.S., 1967. The genus *Palaeoperidinium* Deflandre (Dinophyceae). Grana Palynologica 7, 243–258.

Sarjeant, W.A.S., Stover, L.E., 1978. *Cyclonephelium* and *Tenua*: a problem in dinoflagellate cyst taxonomy. Grana, 17, 47–54.

Saumur, B., Dewing, K., Williamson, M.-C., 2016. Architecture of the Canadian portion of the High Arctic Large Igneous Province and implications for magmatic Ni-Cu-PGE potential. Canadian Journal of Earth Sciences 53, 528-–542.

Schrank, E., 2010. Pollen and spores from the Tendaguru Beds, Upper Jurassic and Lower Cretaceous of southeast Tanzania: palynostratigraphic and paleoecological implications. Palynology 34, 3–42.

Schröder-Adams, C. J., Herrle, J., Embry, A.F., Haggart, J.W., Galloway, J.M., Pugh, A.T., Harwood, D.M. 2014. Aptian to Santonian Foraminiferal Biostratigraphy and Paleoenvironmental Change in the Sverdrup Basin as Revealed at Glacier Fiord, Axel Heiberg Island, Canadian Arctic Archipelago. Palaeogeography, Palaeoclimatology, Palaeoecology 413, 81–100.

Schröder-Adams, C. J., Herrle, J. O., Selby, D., Quesnel, A., Froude, G., 2019. Influence of the High Arctic Igneous Province on the Cenomanian/Turonian boundary interval, Sverdrup Basin, High Canadian Arctic. Earth and Planetary Science Letters 511, 76–88.

Self, S., Schmidt, A., Mather, T.A., 2014. Emplacement charcteristics, time scales, and volcanic gas release rates of continental flood basalt eruptions on Earth. In: Keller, G., Kerr, A.C. (eds.), Volcanism, impacts, and mass extinctions: causes and effects. Geological Society of America special paper 505, The Geologicval Soceity of America, Boulder, pp. 319–337.

Selmeier, A., Grosser, D., 2011, Lower Cretaceous conifer drift wood from Sverdrup Basin, Canadian Arctic Archipelago. Zitteliana 51, 19–35.

1924 Senger, K., Tveranger, J., Ogata, K., Braathen, A., Planke, S., 2014. Late Mesozoic magmatism in
1925 Svalbard: A review. Earth-Science Reviews 139, 123–144.
1926
1927 Singh, C., 1964. Microflora of the Lower Cretaceous Mannville Group, east central Alberta.
1928 Research Council of Alberta, Bulletin, no. 15, 239 p., 29 pl.
1929
1930 Singh, C., 1971. Lower Cretaceous microfloras of the Peace River area, northwestern Alberta.
1931 Research Council of Alberta, Bulletin, no.28, 301–542, pl. 39–80.
1932
1933 Singh, C., 1983. Cenomanian microfloras of the Peace River area, northwestern Alberta.
1934 Research Council of Alberta, Bulletin 44, 322 p., 62 pl.
1935
1936 Sokal, R.R., Rohlf, F.J. 1995. Biometry: The Principles and Practice of Statistics in Biological
1937 Research. 3rd Edition. New York, NY, USA. Freeman, W.H. & Co., 887 pp.
1938
1939 Somers, G., 1952. A preliminary study of the fossil spore content of the Lower Jubilee Seam of
1940 the Sydney Coalfield, Nova Scotia. Nova Scotia Research Foundation, 1–30.
1941
1942 Spicer, R.A., Parrish, J.T., 1986. Palaeobotanical evidence for cool north polar climates in the
1943 middle Cretaceous (Albian–Cenomanian) time. Geology 14, 703–706.
1944
1945 Springer, D.A., Bambach, R.K., 1985. Gradient versus cluster analysis of fossil assemblages: a
1946 comparison from the Ordovician of southwestern Virginia. Lethaia 18, 181–198.

Stott, D.F., 1969. Ellef Ringnes Island, Canadian Arctic Archipelago. Geological Survey of Canada, Paper 68–16, 44 p. (1 sheet).

Stover, L.E. and Evitt, W.R., 1978: Analyses of pre-Pleistocene organic-walled dinoflagellates. Stanford University Publications, Geological Sciences, 15, 300 p.

Stover, L.E., Brinkhuis, H., Damassa, S.P., de Verteuil, L., Helby, R.J., Monteil, E., Partridge, A.D., Powell, A.J., Riding, J.B., Smelror, M., Williams, G.L., 1996. 19. Mesozoic–Tertiary dinoflagellates, acritarchs and prasinophytes. In: Jansonious, J, McGregor, D.C. (eds), Palynology: principles and applications, volume 2, American Association of Stratigraphic Palynologists Foundation, Dallas, U.S.A., 641–750.

Svensen, H., Panke, S., Polozoc, A.G., Schmidbauer, N., Corfu, F., Podladchikov, Y.Y., Jamtveit, B. 2009. Siberian gas venting and the end-Permian environmental crises. Earth and Planetary Science Letters, 277, 490–500.

Svensen, H. H., Torsvik, T.H., Callegaro, S., Augland, L., Heimdal, T.H., Jerram, D.A., Planke, S., Pereira, E. 2017. Gondwana large igneous provinces: plate reconsructions, volcanic basins and sill volumes. Geological Society London Special Publication 463, SP463.7.

Tarduno, J.A., Brinkman, D.B., Renne, P.R., Cottrell, R.D., Scher, H., Castillo, P., 1998. Evidence for extreme climatic warmth from Late Cretaceous Arctic vertebrates. Science 282, 2241–2244.

Tasch, P., McClure, K., Oftedahl, O., 1964. Biostratigraphy and taxonomy of a hystrichosphere–dinoflagellate assemblage from the Cretaceous of Kansas. Micropaleontology 10, 189–206, pl.1–3.

Taugourdeau-Lantz, J., 1988. Stratigraphic implications of early Cretaceous spores and pollen grains in Holes 638B, 638C, and 641C, leg 103, off the Iberian Margin, eastern North Atlantic. In: Boillot, G., Winterer, E.L., Meyer, A.W. (eds.), Proceedings of the Ocean Drilling Program, Scientific Results 103, 419–428.

Tegner, C., Storey, M., Holm, P.M., Thorarinsson, S.B., Zhao, X., Lo, C.-H., Knudsen, M.F., 2011. Magmatism and Eurekan deformation in the High Arctic large igneous province: 40Ar-39Ar age of Kap Washington Group volcanics, North Greenland. Earth and Planetary Science Letters 303, 203–214.

Thiede, D.S., Vasconcelos, P.M., 2010. Paraná flood basalts: Rapid extrusion hypothesis confirmed by new $^{40}Ar/^{39}Ar$ results. Geology 38, 747–750.

Thiergart, F., 1949. Der stratigraphische Wert mezozoischer Pollen und Sporen (The stratigraphic value of Mesozoic pollen and spores). Palaeontographica Abteilung B 89, 1–34, pl. 1–3.

Thomson, P.W., Pflug, H., 1953. Pollen und Sporen des mitteleuropäischen Tertiärs. Gesamtübersicht über die stratigraphisch und paläontologisch wichtigen Formen. Palaeontographica, Abteilung B 94, 1–138, pl.1–16.

Thorsteinsson, R. 1971. Geology, Eureka Sound North, District of Franklin. Geological Survey of Canada Map 1302A, https://doi.org/10.4095/109125.

Thorsteinsson, R., 1974. Carboniferous and Permian stratigraphy of Axel Heiberg Island and western Ellesmere Island, Canadian Arctic Archipelago. Geological Survey of Canada Bulletin 224, 115 p (22 sheets).

Tozer, E.T., 1963. Mesozoic and Tertiary stratigraphy, western Ellesmere Island and Axel Heiberg Island, District of Franklin. Geological Survey of Canada, Paper 63–30, 42 p.

Tozer, E.T., Thorsteinsson, R., 1964. Western Queen Elizabeth Islands, Arctic Archipelago. Geological Survey of Canada, Memoir 332, 242 p (2 sheets).

Traverse, A., 2007. Palynological Laboratory Techniques, in: Paleopalynology, Second Edition. Topics in Geobiology Series, Volume 28. Springer-Verlag, New York, pp. 615–772.

Tschudy, R.H., Tschudy, B.D., 1986. Extinction and survival of plant life following the Cretaceous/Tertiary boundary event, western interior, North America. Geology 14, 667–670.

Tschudy, R.H., Pillmore, C.L., Orth, C.J., Gilmore, J.S., Knight, J.D., 1984. Disruption of the terrestrial plant ecosystem at the Cretaceous–Tertiary boundary, Western Interior. Science 225, 1030–1032.

Tullius, D.N., Leier, A., Galloway, J.M., Embry, A.F., Pedersen, P.K., 2014. Sedimentology and stratigraphy of the Lower Cretaceous Isachsen Formation; Ellef Ringnes Island, Sverdrup Basin, Canadian Arctic Archipelago. Journal of Marine and Petroleum Geology 57, 135–151.

Vajda, V., Bercovici, A., 2014. The global vegetation pattern across the Cretaceous–Paleogene mass extinction interval: a template for other extinction events. Global and Planetary Change 122, 29–49.

Valensi, L., 1955. Sur quelques microorganismes des silex crétacés du Magdalénien de Saint-Amand (Cher) (On some microorganisms of Cretaceous flint from the Magdalenian of Saint-Amand (Cher). Bulletin de la Société géologique de France (Bulletin of the Geological Society of France), 6e série 5, 35–40.

van de Schootbrugge, B., Quan, T.M., Lindström, S., Püttmann, W., Heunisch, C., Pross, J., Fiebig, J., Petschick, R., Röhling, H.-G., Richoz, S., Rosenthal, Y., Falkowski, P.G., 2009. Floral changes across the Triassic/Jurassic boundary linked to floodflood basalt volcanism. Nature Geoscience 2, 589–594.

Venkatachala, B.S., Kar, R.K., 1970. Palynology of Mesozoic sediments of Kutch, W. India. 10. Palynological zonation of Katrol (Upper Jurassic) and Bhuj (Lower Cretaceous) sediments in Kutch, Gujarat. The Palaeobotanist 18, 75–86.

Venkatachala, B.S., Kar, R.K., Raza, S., 1969. Palynology of the Mesozoic sediments of Kutch, W. India. 3. Morphological study and revision of the spore genus *Trilobosporites* Pant ex Potonié 1956. The Palaeobotanist 17, 123–126, pl. 1.

Vickers, M.L., Price, G.D., Jerrett, R.M., Watkinson, M., 2016. Stratigraphic and geochemical expression of Barremian-Aptian global climate change in Arctic Svalbard. Geosphere 12, 1594–1605.

Vickers, M., Price, G.D., Jerrett, R.M., Sutton, P., Watkinson, M.P., FitzPatrick, M., 2019. The duration and magnitude of Cretaceous cool events: evidence from the northern latitudes. Geological Society of America Bulletin 131, 1979–1994.

Wall, J.H., 1983. Jurassic and Cretaceous foraminiferal biostratigraphy in the eastern Sverdrup Basin, Canadian Arctic Archipelago. Canadian Petroleum Geology 31, 247–281.

Wang, Y., Huang, C., Sun, B., Quan, C., Wu, J., Lin, Z., 2014. Paleo-CO2 variation trends and the Cretaceous greenhouse climate. Earth-Science Reviews 129, 136–147.

Waylett, D.C., Embry, A.F., 1992. Hydrocarbon loss from oil and gas fields of the Sverdrup Basin, Canadian Arctic Islands. In: Vorren, T.O., Bergsager, E., Dahl-Stamnes, Ø.A., Holter, E.,

Johansen, B., Lie, E., Lund, T.B. (eds.), Arctic Geology and Petroleum Potential. Norwegian Petroleum Society Special Publication 2, Elsevier, Amsterdam, 205–216.

Weissert, H., 1989. C-isotope stratigraphy, a monitor of paleoenvironmental change: A case study form the early Cretaceous. Surveys in Geophysics 10, 1–61.

Wetzel, O., 1933. Die in organischer Substanz erhaltenen Mikrofossilien des baltischen Kreide-Feuersteins mit einem sediment-petrographischen und stratigraphischen Anhang (The organic fossils of the Baltic chalk flint with a sediment-petrographic and stratigraphic appendix). Palaeontographica Abteilung A, 78, 1–110, pl.1–7.

Weyland, H., Greifield, W., 1953. Über strukturbietende Blätter und pflanzliche Mikrofossilien aus den Untersenonen Tonen der Gegend von Quedlinburg (About structure-offering leaves and plant microfossils from the Untersenonen clays of the Quedlinburg area). Palaeontographica B 95, 30–52.

White, H.H., 1842. On fossil *Xanthidia*. Microscopical Journal, London, 11, 35–40, pl.4.

Wilson, L.R., Webster, R.M., 1946. Plant microfossils from a Fort Union Coal of Montana. American Journal of Botany, 33, 271–278.

Wodehouse, R.P., 1933. Tertiary pollen: II, the oil shales of the Green River Formation. Bulletin of the Torrey Botanical Club 60, 479–524.

Woodward, F.I., 1998. Vegetation-climate feedbacks in a greenhouse world. Philosophical Transactions Royal Society London B, Biological Sciences 353, 29–39.

Wynne, P.J., Irving, E., Osadetz, K.G., 1988. Paleomagnetism of Cretaceous volcanic rocks of the Sverdrup Basin – magnetostratigraphy, paleolatitudes, and rotations. Canadian Journal of Earth Science 25, 1220–1239.

Yun H, 1981. Dinoflagellaten aus der Oberkreide (Santon) von Westfalen (Dinoflagellates from the Upper Chalk (Santon) of Westphalia). Palaeontographica, Abteilung B 177, 1–89, pl.1–16.

Figure 1. (colour online) Geologic map of the Sverdrup Basin (after Dewing et al. 2007) showing the location of studied Glacier Fiord succession on Axel Heiberg Island

Figure 2. (colour online) Mesozoic lithostratigraphy of the Sverdrup Basin (after Hadlari et al. 2016). The Geological Time Scale v 2020 for Jurassic and Cretaceous systems (Hesselbo et al. 2020; Gale et al., 2020) is used. Note that ages of intrusive rocks should be younger than the strata that they intrude, and that detrital zircon ages can be older than the rocks in which they occur. For detailed summaries and discussions of age determinations of Lower Cretaceous strata, see Galloway et al. (2013, 2015, 2019), Schröder-Adams et al. (2014), and Herrle et al. (2015)

Figure 3. (colour online) Lithostratigraphic section of the Isachsen Formation measured at Glacier Fiord, Axel Heiberg Island, showing stratigraphic positions of samples collected and analyzed for palynology (Table 1), sequence stratigraphy (after Galloway et al., 2015), facies associations (after Tullius et al., 2014), and informal palynozones based on stratigraphically constrained cluster analysis of pollen of obligately terrestrial pollen and spores

Figure 4a. (colour online) Photographs of dinocysts identified in Isachsen Formation preparations from samples collected from Glacier Fiord. Photographs of the dinocysts have been cleaned of extraneous material, but the images of the specimens have not been altered beyond brightness and contrast adjustments. Sample number, GSC curation number (C-number), GSC Calgary Palynology Laboratory preparation number (P-number),

Government of Nunavut specimen number (pending), microscope and England Finder coordinates, and magnification:

A. *Callaiosphaeridium* sp. A, B-36, C-548345, P-5231-39H, 087 x 0815, EF H24-3, x40P. This is a form of *Callaiosphaeridium* with cingular processes significantly wider that those of *Callaiosphaeridium assymmetricum*.

B. *Catastomocystis* sp. A, B-36, C-548345, P-5231-39H, 198 x 0773, EF T19-4, x40P. A form of *Catastomocystis* similar to *Catastomocystis spinosa* but with a smooth outline, without spines.

C. *Chlamydophorella nyei*, B-34, C-548343, P-5231-37H, 104 x 0884, EF K31-0/1, x40P.

D. Dinocyst gen et sp. Indet, B-35, C-548344, P-5231-38H, 158 x 0729, EF P15-0/3, x40P.

E. *Chlamydophorella trabeculosa*, B-35, C-548344, P-5231-38I, 181 x 0942, EF S37-0/1, x40P.

F. *Kiokansium unituberculatum*, B-34, C-548343, P-5231-37H, 195 x 0941, EF T37-0, x40P.

G. *Kiokansium unituberculatum*, B-36, C-548345, P-5231-39H, 052 x 0719, EF D14-0/3, x40P.

H. *Kleithriasphaeridium cooksoniae*, B-34, C-548343, P-5231-37H, 100 x 0751, EF J17-2, x40P.

I. ?*Muderongia crucis*, B-36, C-548345, P-5231-39H, 056 x 0724, EF E14-2, x40P.

J. ?*Muderongia crucis*, B-37, C-548346, P-5231-40H, 135 x 0725, EF N14-0/2, x40P

K. *Nyktericysta* sp. A, B-38, C-548347, P-5231-41H, 187 x 0917, EF S34-4, x40P. A *Nyktericysta* with a coarsely reticulate periphragm.

L. *Oligosphaeridium albertense*, B-34, C-548343, P-5231-37H, 187 x 0739, EF S16-0/1, x40P.

M. *Oligosphaeridium anthophorum*, B-35, C-548344, P-5231-38H, 066 x 0801, EF F22-0/2, x40P.

N. *Oligosphaeridium asterigerum*, B-34, C-548343, P-5231-37H, 117 x 0899, EF L32-4, x40P.

O. *Oligosphaeridium diluculum*, B-36, C548345, P5231-39H, 087 x 0848, EF H27-0, x40P.

P. *Oligosphaeridium diluculum*, B-36, C-548345, P-5231-39H, 197 x 0868, EF T29-3/4, x40P.

Q. *Oligosphaeridium porosum*, B-35, C-548344, P-5231-38H, 092 x 0966, EF J39-2, x40P.

R. *Oligosphaeridium porosum*, B-35, C-548344, P-5231-38H, 197 x 0827, EF T25-0, x40P.

S. *Oligosphaeridium pulcherrimum*, B-36, C-548345, P-5231-39H, 135 x 0679, EF N10-3, x40P, high focus.

T. *Oligosphaeridium pulcherrimum*, B-36, C-548345, P-5231-39H, 135 x 0679, EF N10-3, x40P, low focus.

Figure 4b. (colour online) Photographs of dinocysts identified in Isachsen Formation preparations from samples collected from Glacier Fiord. Photographs of the dinocysts have been cleaned of extraneous material, but the images of the specimens have not been altered beyond brightness and contrast adjustments. Sample number, GSC curation number (C-number), GSC Calgary Palynology Laboratory preparation number (P-number), Government of Nunavut specimen number (pending), microscope and England Finder coordinates, and magnification:

A. *Palaeoperidinium cretaceum*, B-36, C-548345, P-5231-39H, 118 x 0895, EF L32-0, x40P.

B. *Psaligonyaulax* sp., B-35, C-548344, P-5231-38H, 108 x 0767, EF K19-3, x40P.

C. *Pseudoceratium pelliferum*, B-36, C-548345, P-5231-39H, 160 x 1010, EF Q44-1, x40P.

D. *Pseudoceratium pelliferum*, B-37, C-548346, P-5231-40H, 079 x 0951, EF G38-0, x40P.

E. *Pseudoceratium nudum*, B-36, C-548345, P-5231-39H, 201 x 0910, EF U33-2, x40P. (Species here retained in *Pseudoceratium*.)

F. *Pseudoceratium nudum*, B-37, C-548346, P-5231-40H, 146 x 0825, EF O25-0/1, x40P.

G. *Pseudoceratium nudum*, B-37, C-548346, P-5231-40H, 137 x 0870, EF N29-4, x40P.

H. *Sirmiodinium grossii*, B-34, C-548343, P-5231-37H, 137 x 0940, EF N37-3, x40P.

I. *Subtilisphaera senegalensis*, B-38, C-548347, P-5231-41H, 124 x 0884, EF M31-0/1, x40P.

J. *Tanyosphaeridium xanthiopyxides*, B-35, C-548344, P-5231-38I, 144 x 0980, EF O41-0, x40P.

K. *Tenua hystrix*, B-36, C-548345, P-5231-39H, GSC 141134, 084 x 0818, EF G24-3/4, x40P.

L *Tenua scabrosa*, B-35, C-548344, P-5231-38H, GSC 141135, 108 x 0979, EF K41-3, x40P.

M. *Nyktericysta vitrea*, B-35, C-548344, P-5231-38H, GSC 141136, 102 x 0901, EF K31-0/1, x40P.

N. *Trichodinium* sp., B-35, C-548344, P-5231-38H, GSC 141137, 065 x 0811, EF F23-2, x40P.

O. *Trichodinium* sp., B-38, C-548347, P-5231-41H, GSC 141138, 196 x 0971, EF T40-0/3, x40P.

P. *Tenua scabrosa*, B-35, C-548344, P-5231-38H, GSC 141139, 137 x 0916, EF N34-0, x40P.

Q. *Nyktericysta*? *vitrea*, B-35, C-548344, P-5231-38H, GSC 141140, 119 x 0772, EF L19-2/4, x40P.

R. *Vesperopsis longicornis*, B-37, C-548346, P-5231-40H, GSC 141141, 189 x 0922, EF T35-1, x40P.

S. *Vesperopsis longicornis*, B-38, C-548347, P-5231-41H, GSC 141142, 198 x 0770, EF T19-3/4, x40P.

T. *Vesperopsis* sp. A, B-36, C-548345, P-5231-39H, GSC 141143, 168 x 0804, EF Q23-3, x40P.

Figure 5. (colour online) Pollen and spores photographed using differential interference contrast and oil immersion preserved in Isachsen Formation preparations from samples collected from Glacier Fiord. Sample number, GSC-C curation number (C-number), GSC-Calgary Palynology Laboratory preparation number (P-number), Government of Nunavut Specimen Number (pending), and England Finder coordinates where available:

A. *Classopollis classoides*, B-33b, C-548342, P5231-36B, W24/2.

B. *Cycadopites follicularis*, B-3, C-548317, P5231-11B, V13/4.

C. *Eucommiidites troedssonii*, B-38, C-548347, P5231-41E, M12/2.

D. *Perinopollenites elatoides*, B-3, C-54317, P5231-11B, U15/3.

E. *Aequitriradites verrucosus*, B-24, C-548332, P5231-26B, R38/3 (proximal surface in focus).

F. *Aequitriradites verrucosus*, B-24, C-548332, P5231-26B, R38/3 (distal surface in focus).

G. *Stereisporites antiquasporites*, B-31, C-548339, P5231-33b, M36/4.

H. *Antulisporites distaverrucosus*, B-3, C-548342, P5231-36B, GTA-B33b, J28/3.

I. *Baculatisporites comaumensis*, B-3, C-548317, P5231-11B, V12/2.

J. *Cicatricosisporites hughesii*, B-48, C-548357, P5231-51B.

K. *Ruffordiaspora australiensis*, B-41, C-548350, P5231-44B (proximal surface in focus).

L. *Ruffordiaspora australiensis*, B-41, C-548350, P5231-44B (distal surface in focus).

M. *Dictyophyllidites harrisii*, B-33b, C-548342, P5231-36B, N21/4.

N. *Gleicheniidites senonicus*, B-3, C-548317, P5231-11B, R12/2.

O. *Cicatricosisporites pseudotripartitus*, B-36, C-548345, P5231-39B, no England finder coordinates.

P. *Ruffordiaspora australiensis*, B-11, C-548219, P5231-13B, no England finder coordinates.

Q. *Trilobosporites*, B-9, C-548317, P5231-11B, no England Finder coordinates.

R. *Ischyosporites disjuncta*, B-3, C-548317, P5231-11B, V9/3.

S. *Punctatisporites scabratus*, B-33b, C-548342, P5231-36B, no England Finder coordinates.

T. *Punctatisporites scabratus*, B-19, C-548327, P5231-21B, no England Finder coordinates.

Figure 6. (colour online) Q- and R-mode cluster analysis of relative abundance data and Non-Metric Multidimensional Scaling (NMDS) bi-plot of square root transformed relative

abundance data of palynomorphs with affinities to plant order (with exceptions explained in the text), algae and protists (*Tasmanites*, *Pediastrum*, *Pterospermella* and undifferentiated dinocysts), acritarchs (*Veryhachium*, *Micrhystridium*), and other NPP (*Sigmopollis* and *Chomotriletes*) preserved in preparations of Isachsen Formation samples collected from Glacier Fiord. Pie charts are colour coded to show the proportion of Q-mode clusters A-D in the samples of the Paterson Island, Rondon, and Walker Island members of the Isachsen Formation. Taxa in each order are shown in Suppl. 3

Figure 7. (colour online) Stratigraphic diagram of the relative abundance of taxa at the order level composing each cluster determined from Q-mode cluster analysis (Fig. 6; Suppl. 3). Stratigraphically constrained incremental sum of squares cluster analysis (CONISS; Grimm, 1987) of square root transformed relative abundance of palynomorphs at the order level is used in conjunction with visual inspection to delineate informal palynomorph stratigraphic zones for each section (zones 1–4) (2 column formatting). Dinocysts and NPP are not included in the CONISS

Figure 8. (colour online). Summary diagram showing the relative abundance of spores, pollen, and non-pollen palynomorphs (NPP), stratigraphic palynological zones delineated using CONISS (see Fig. 7), palynological events, HALIP events, and inferred paleoclimate during deposition of the Isachsen Formation. References for HALIP ages are (1) Evenchick et al. (2015); (2) Dockman et al. (2018). References for volcanic flows in text

Table 1. Samples analyzed for quantitative and qualitative palynology from Isachsen Formation, Glacier Fiord, Axel Heiberg Island

Lithostratigraphy	Sample name[a]	Meters above base of Isachsen Formation[b]	C-number[c]	P-number[d]	NUPB loan number[e]
Walker Island Member	2011-GTA-B-56	484	C-548365	P-523159[g]	NUPB 831
	2011-GTA-B-55	478	C-548364	P-523158[g]	NUPB 832
	2011-GTA-B-54	473	C-548363	P-523157[g]	NUPB 833
	2011-GTA-B-53	464	C-548362	P-523156[g]	NUPB 834
	2011-GTA-B-52	441.5	C-548361	P-523155[g]	NUPB 835
	2011-GTA-B-51	418.5	C-548360	P-523154[g]	NUPB 836
	2011-GTA-B-50	416	C-548359	P-523153[g]	NUPB 837
	2011-GTA-B-57	410	C-495034	P-523160[g]	NUPB 838
	2011-GTA-B-49	402	C-548358	P-523152[g]	NUPB 839
	2011-GTA-B-48	384	C-548357	P-523151[g]	NUPB 840
	2011-GTA-B-47	375.5	C-548356	P-523150[g]	NUPB 841
	2011-GTA-B-46	373	C-548355	P-523149[g]	NUPB 842
	2011-GTA-B-45	363	C-548354	P-523148[g]	NUPB 843
	2011-GTA-B-44	351	C-548353	P-523147[g]	NUPB 844
	2011-GTA-B-43	345	C-548352	P-523146[f]	NUPB 845
	2011-GTA-B-42	344	C-548351	P-523145[g]	NUPB 846
	2011-GTA-B-41	331.5	C-548350	P-523144[g]	NUPB 847
	2011-GTA-B-40	329	C-548349	P-523143[g]	NUPB 848
	2011-GTA-B-39	324.5	C-548348	P-523142[g]	NUPB 849
Rondon Member	2011-GTA-B-38	303.5	C-548347	P-523141[g]	NUPB 850
	2011-GTA-B-37	299.5	C-548346	P-523140[g]	NUPB 851
	2011-GTA-B-36	298	C-548345	P-523139[g]	NUPB 852
	2011-GTA-B-35	291	C-548344	P-523138[g]	NUPB 853
Paterson Island Member	2011-GTA-B-34	278.5	C-548343	P-523137[g]	NUPB 854
	2011-GTA-B-33b	275.5	C-548346	P-523136[f]	NUPB 855
	2011-GTA-B-33a	268.7	C-548341	P-523135[g]	NUPB 856
	2011-GTA-B-32	266.5	C-548340	P-523134[f]	NUPB 857
	2011-GTA-B-31	255.5	C-548339	P-523133[g]	NUPB 858
	2011-GTA-B-30	222	C-548338	P-523132[f]	NUPB 859
	2011-BTA-B-29	221	C-548337	P-523131[f]	NUPB 860
	2011-GTA-B-28	212.7	C-548336	P-523130[f]	NUPB 861
	2011-GTA-B-27	244.5	C-548335	P-523129[g]	NUPB 862
	2011-GTA-B-26	243	C-548334	P-523128[g]	NUPB 863
	2011-GTA-B-25	241.5	C-548333	P-523127[g]	NUPB 864
	2011-GTA-B-24	240	C-548332	P-523126[g]	NUPB 865
	2011-GTA-B-11	112	C-548319	P-523113	NUPB 866
	2011-GTA-B-9	74.5	C-548317	P-523111	NUPB 867
	2011-GTA-B-1	5	C-548309	P-523103	NUPB 868

[a]GSC code for Jennifer Galloway is GTA; [b]0 m is base formational contact with underlying Deer Bay Formation; [c]GSC Palynology Laboratory Preparation Number; [d]GSC Curation Number; [e]Nunavut Curation Number, Canadian Museum of Nature Registration Number NL2020-001 on loan from 05/03/2020 to 31/03/2021;[f]qualitatively analyzed for dinocysts (+45 µm size fraction) but not included in quantitative analyses of terrestrial pollen and spores; [g]qualitatively analyzed for dinocyst identification and included in quantitative analyses of terrestrial pollen and spores

Table 2: Age information of the dinocyst taxa identified in the Rondon Member of the Isachsen Formation at Glacier Fiord

Taxon[a]	Age
Batioladinium daviesii	Type is late Valanginian
Callaiosphaeridium	*Callaiosphaeridium asymmetricum* ranges from early Hauterivian to early Campanian according to Costa and Davey (1992); and early Hauterivian to late Campanian according to Stover et al. (1996).
Catastomocystis	The type *Catastomocystis spinosa* is early Cenomanian.
Chlamydophorella trabeculosa	Early Hauterivian to late Aptian according to Costa and Davey (1992) and Stover et al (1996).
Kiokansium unituberculatum	LO[b] is late Cenomanian according to Costa and Davey (1992).
Kleithriasphaeridium cooksoniae	Type is late Albian. Range is early Aptian to top Cenomanian according to Stover et al. (1996).
Muderongia crucis	*Muderongia crucis*/*tetracantha* LO plotted as early Barremian by Costa and Davey (1992). Range of *Muderongia tetracantha* is early Valanginian to early Barremian according to Stover et al. (1996).
Nyktericysta and *Vesperopsis*	The range of *Vesperopsis* spp. is recorded as late Barremian to early Cenomanian by Stover et al. (1996). LO of *Nyktericysta tripenta* recorded as late Albian by Fensome et al. (2008).
Oligosphaeridium albertense	LO is early Cenomanian according to Costa and Davey (1992).
Oligosphaeridium diluculum	FO[c] is plotted as Ryazanian in Costa and Davey (1992) and questionable from early Valanginian upwards.
Pseudoceratium pelliferum	Range is late Ryazanian to top Barremian according to Costa and Davey (1992); and late Ryazanian to early Aptian in Stover et al. (1996).
Sirmiodinium grossii	Tentatively goes into early Aptian according to Costa and Davey (1992). LO plotted as early Aptian in Stover et al (1996).
Tanyosphaeridium xanthiopyxides	The possibly synonymous species *Tanyosphaeridium variecalamum* was plotted as Valanginian to Maastrichtian in Stover et al. (1996).
Tenua hystrix	Based on discussion in Fensome et al (2019a), this species ranges from Berriasian to Maastrichtian.
Tenua scabrosa	According to Fensome et al. (2019a), the provisional range of this species is late Hauterivian to Cenomanian.

[a]see Appendix A for taxonomic authority; [b]LO-last occurrence; [c]FO-first occurrence

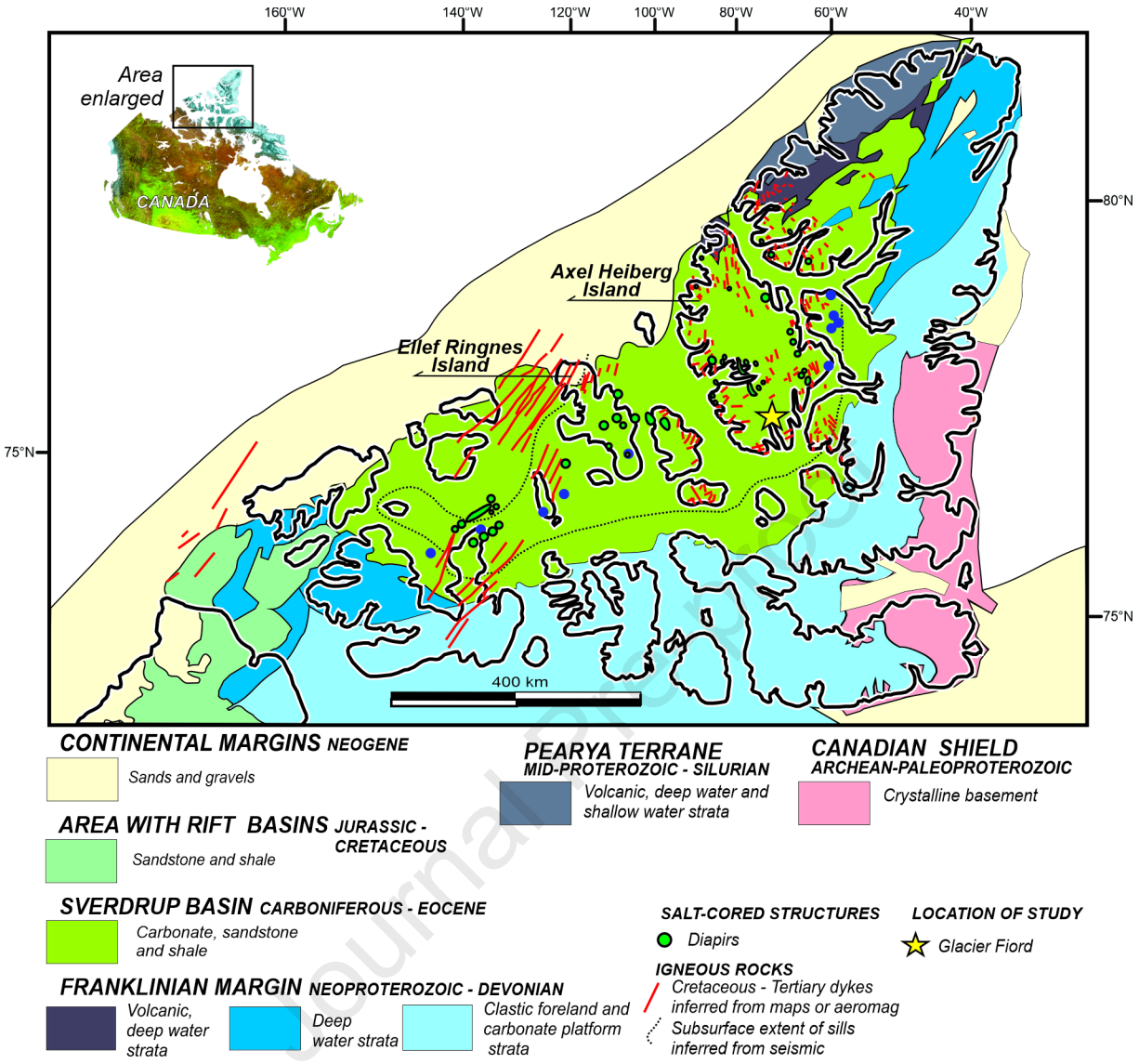

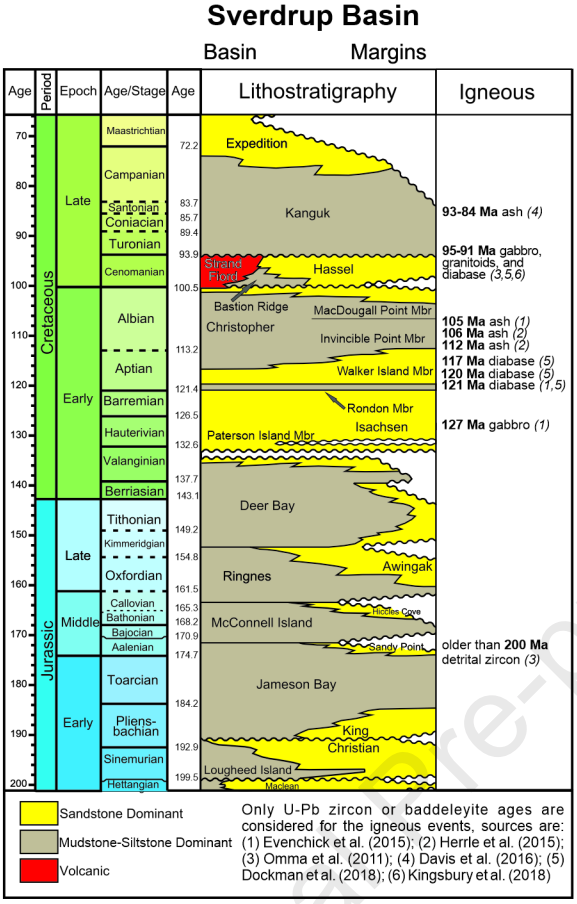

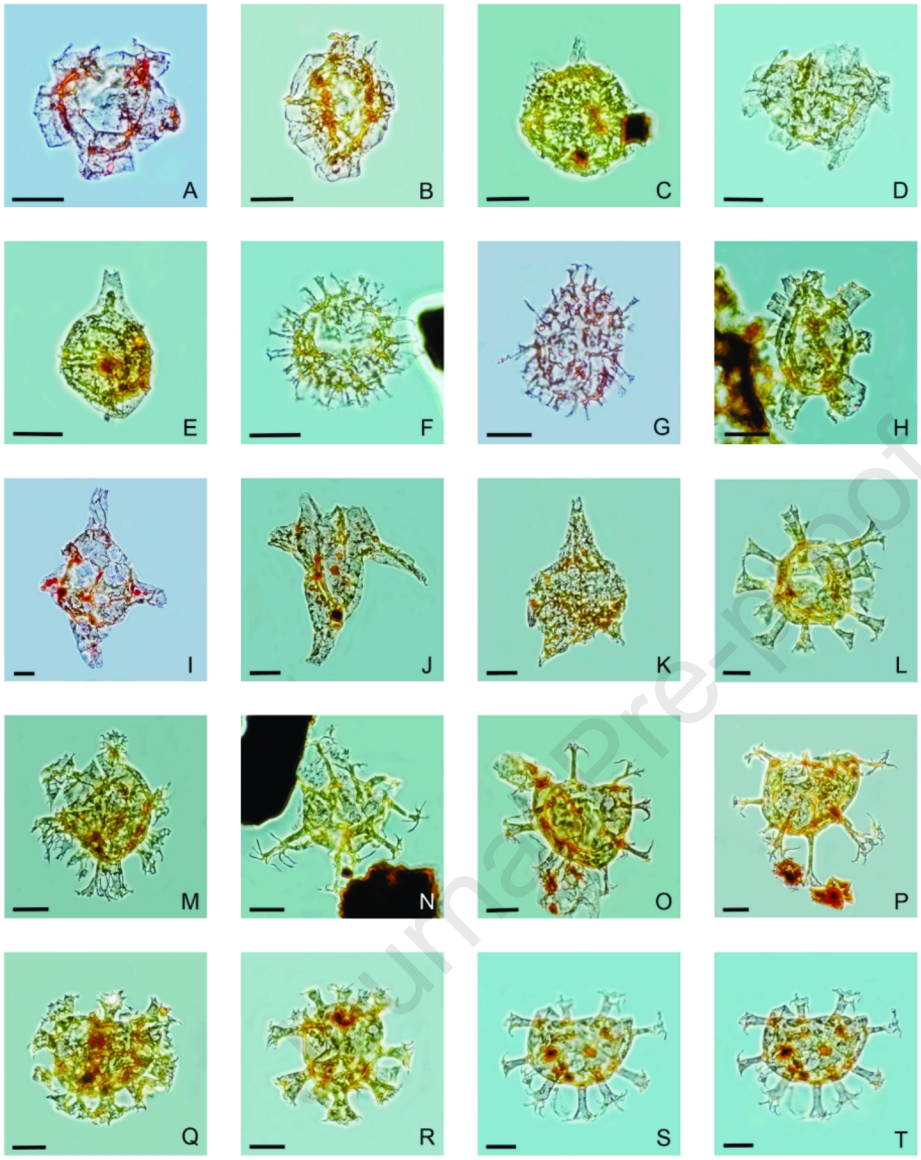

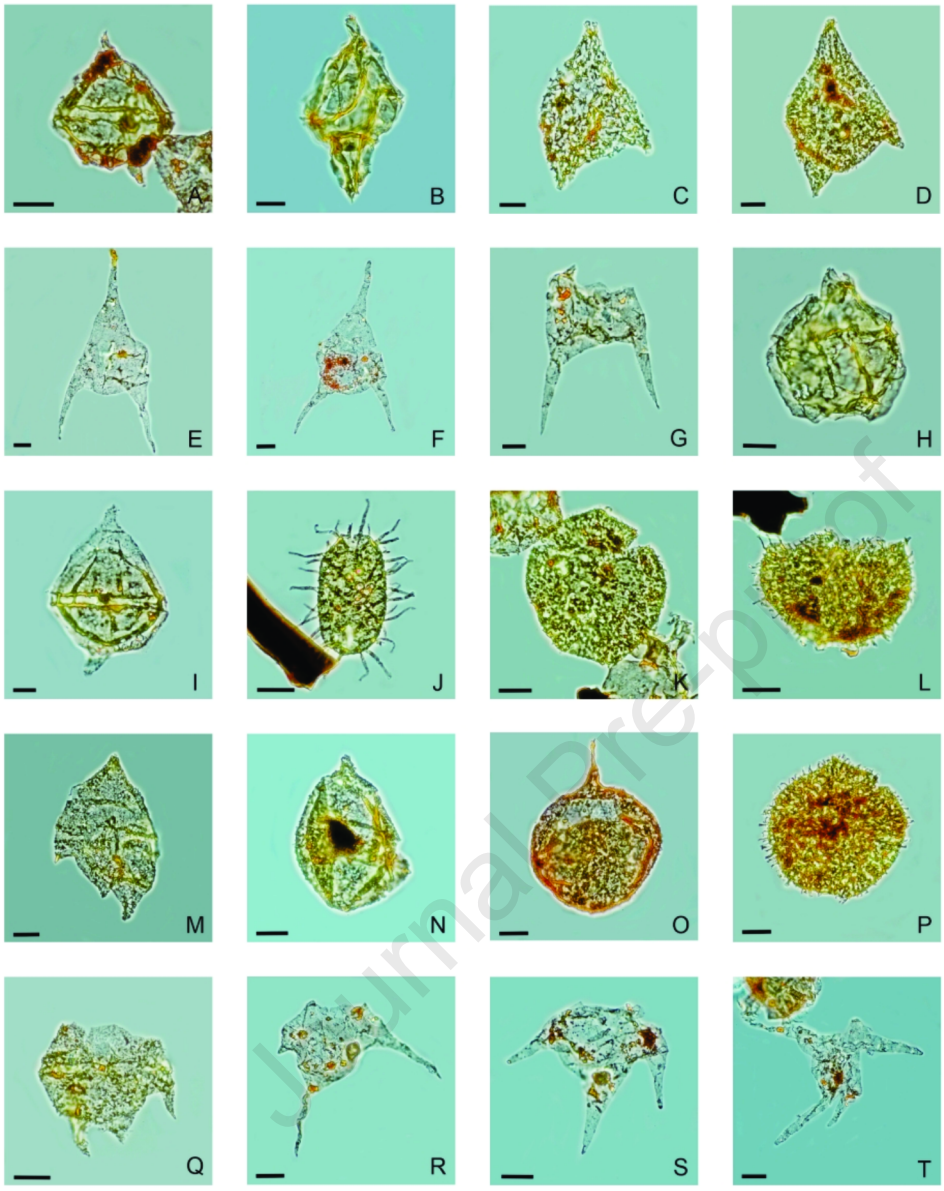

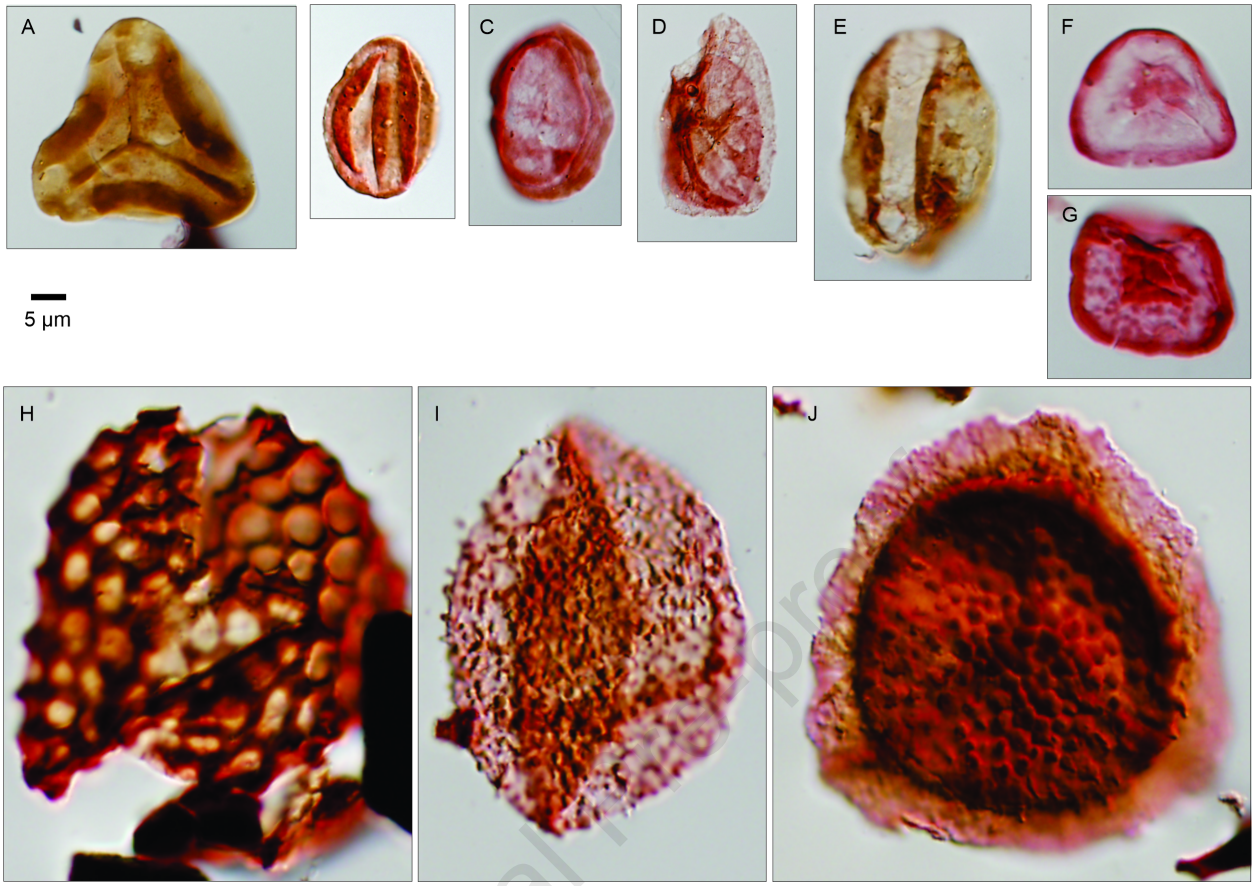

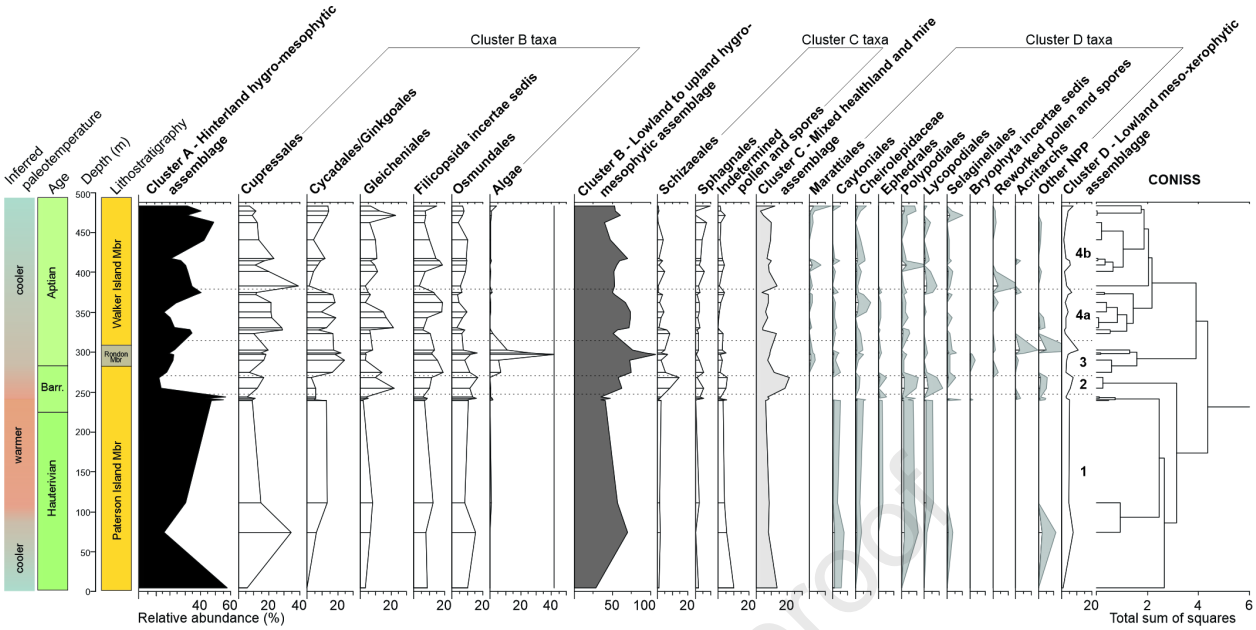

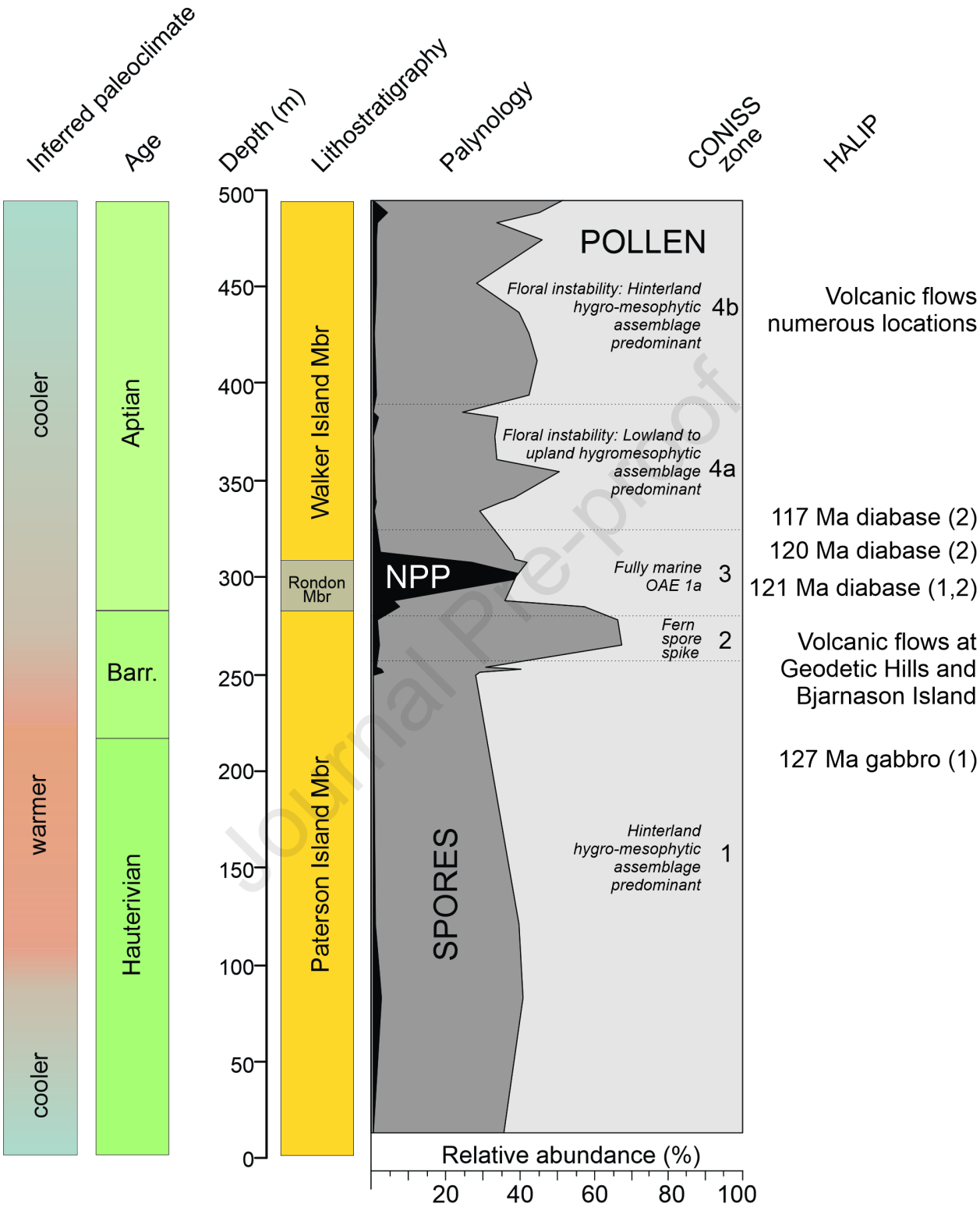

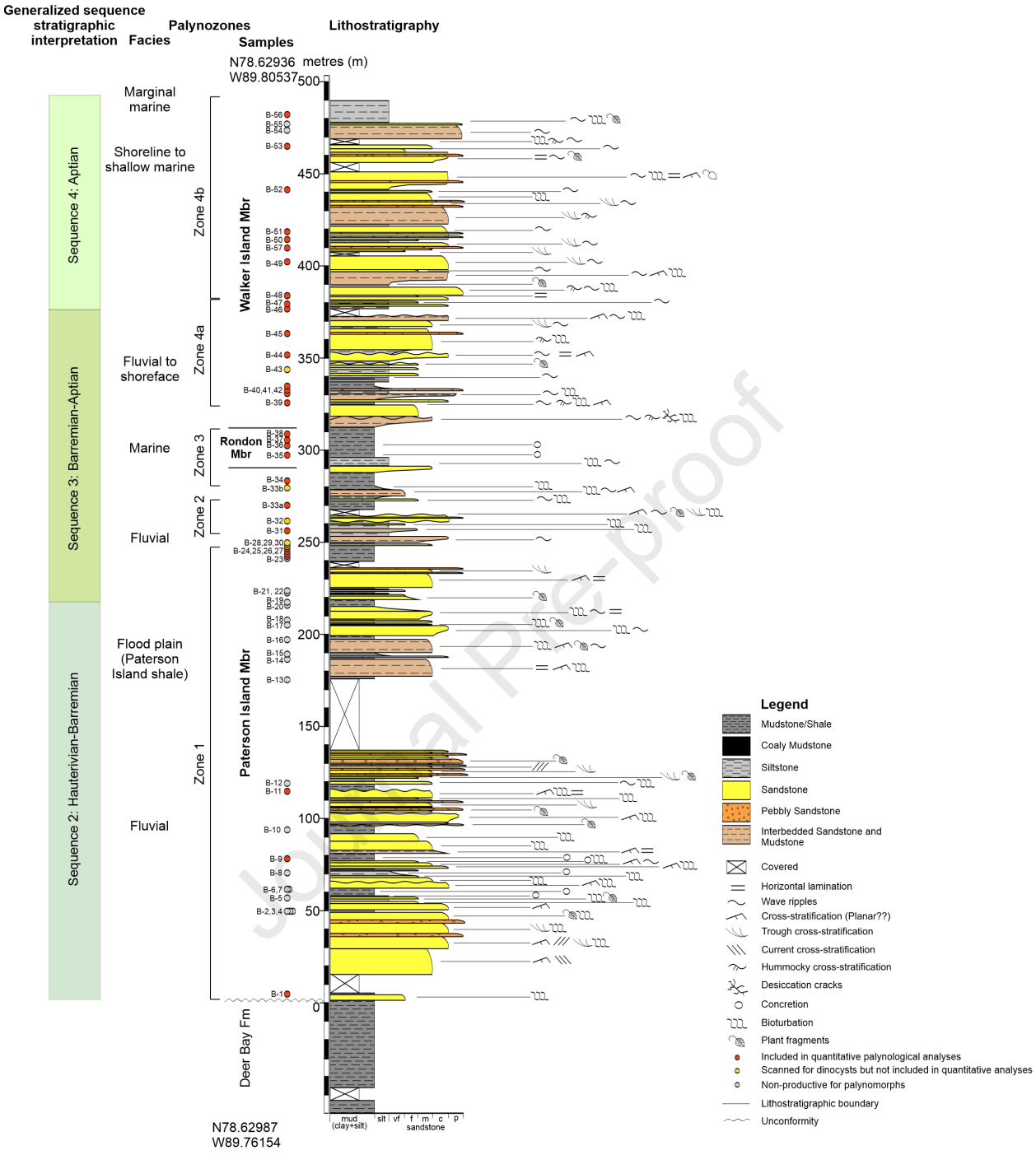

Natural Resources Canada

Geological Survey of Canada (Calgary)
3303-33rd Street N.W., Calgary Alberta T2L 2A7

Telephone: (403) 292-7000
URL: http://www.nrcan.gc.ca

Ressources naturelles Canada

Commission géologique du Canada (Calgary)
3303, 33e Rue N.-O. Calgary Alberta T2L 2A7

Téléphone: (403) 292-7000
URL: http://www.rncan.gc.ca

June 07, 2020

Jennifer Galloway, Ph.D.

Research Scientist / Chercheuse scientifique
Chief Paleontologist / paléontologue en chef
Geological Survey of Canada (GSC) Commission géologique du Canada
Natural Resources Canada (NRCan) Ressources naturelles Canada
Adjunct Research Professor, Department of Earth Sciences, Carleton University, Ottawa, Ontario
Adjunct Assistant Professor, Department of Geosciences, University of Calgary, Calgary, Alberta
Adjunct Professor, Department of Geology, Brandon University, Brandon, Manitoba

3303 - 33 Street N.W. Calgary, AB, T2L 2A7, Canada

☎ (587) 892-2892 🖷 (403) 292-4961 jennifer.galloway@canada.ca

Dear Editor,

Please find enclosed a manuscript submitted for consideration of publication in *Cretaceous Research* by Galloway et al. entitled:

High Arctic Large Igneous Province Impacts on Arctic forests during the Hauterivian to early Aptian

All work in this manuscript represents original contributions that are not being considered for publication elsewhere. All previously published work cited in this manuscript is acknowledged. Each co-author of this manuscript has contributed substantially to this work and approve of its final submission to *Cretaceous Research.*

We declare no conflict of interest.

Our CRediT author statement is as follows **Galloway:** conceptualization, methodology, formal analysis, investigation, resources, data curation, writing-original draft preparation, project administration, visualization, project administration, funding acquisition **Fensome:** methodology, formal analysis, investigation, data curation, writing-original draft preparation, visualization **Swindles:** methodology, formal analysis, writing-review and editing **Hadlari:** methodology, investigation, formal analysis, writing-original draft preparation **Fath:** investigation, data curation, writing-review and editing **Schröder-Adams:** conceptualization, methodology, investigation, funding acquisition, writing-review and editing **Herrle:** conceptualization methodology, investigation, funding acquisition, writing-review and editing **Pugh:** investigation, writing-review and editing

Sincerely,

Jennifer Galloway